



*Sede di Napoli*



**EUROPEAN SCHOOL OF MOLECULAR MEDICINE**  
**SEDE DI NAPOLI**  
**UNIVERSITA' DEGLI STUDI DI NAPOLI "FEDERICO II"**

**Ph.D. in Molecular Medicine – Ciclo II/XX**  
**Human Genetics**



**“Functions of the Krüppel-like Factor 7 protein in cellular differentiation and neuronal morphogenesis”**

Tutor:

Prof. Francesco Ramirez

Internal Supervisor:

Prof. Lucio Pastore

External Supervisor:

Prof. Stefano Stifani

Coordinator:

Prof. Francesco Salvatore

Ph.D. student:

Dr. Massimiliano Caiazzo

**Academic Year: 2008-2009**

# INDEX

<b>ABBREVIATIONS INDEX</b> .....	4
----------------------------------	---

## **CHAPTER 1 – INTRODUCTION**

1.1	Transcription factors .....	6
1.2	The zinc finger transcription factors family .....	6
1.3	The Krüppel-like transcription factors .....	7
1.4	The Krüppel-like Factor 7 .....	9
1.4.1	The Krüppel-like Factor 7 expression .....	11
1.4.2	The Krüppel-like Factor 7 functional role .....	13
1.4.2.1	KLF7 molecular function .....	13
1.4.2.2	KLF7 biological function .....	13
1.5	Neural stem cells .....	16
1.5.1	NSC location in the embryonic and adult mammalian CNS .....	16
1.5.2	An <i>In vitro</i> tool to study NSC: neurospheres .....	17
1.6	The dopaminergic system .....	17
1.6.1	Development of dopaminergic neurons .....	20
1.6.1.1	Early midbrain patterning and induction of DA precursors .....	21
1.6.1.2	Differentiation of postmitotic DA neurons .....	21
1.6.1.3	Maturation and survival of the dopaminergic phenotype .....	22
1.7	Thesis project aim .....	23

## **CHAPTER 2 – MATERIALS AND METHODS**

2.1	Cell cultures .....	25
2.1.1	PC12 cells .....	25
2.1.2	ES cells.....	25
2.1.2.1	ES cells neuronal differentiation.....	25
2.1.2.2	ES cells cardiogenic differentiation .....	26
2.1.3	Mouse embryonic fibroblasts (MEF).....	26
2.1.3.1	MEF preparation .....	26

2.1.3.2	MEF adipogenic differentiation.....	27
2.1.3.3	Oil red O staining.....	27
2.1.3.4	MEF osteogenic differentiation .....	28
2.1.3.5	Alizarin red S staining .....	28
2.1.4	Neurospheres.....	28
2.1.4.1	Neurospheres neural differentiation.....	29
2.1.4.2	Neurospheres assay.....	29
2.2.	Cell transfection .....	29
2.2.1	RNAi.....	30
2.3	Animal and dissections .....	30
2.3.1	Mice genotyping .....	30
2.3.1.1	PCR analysis .....	31
2.4	RNA isolation and real time RT-PCR analysis.....	34
2.5	Western blot analysis .....	34
2.6	Immunocytochemical analysis.....	35
2.7	Immunohistochemical analysis.....	36

### **CHAPTER 3 – RESULTS**

3.1	Expression profile of <i>Klf7</i> in proliferating and differentiated PC12 and ES cells.....	38
3.2	<i>Klf7</i> gene silencing in PC12 cells .....	39
3.3	<i>Klf7</i> gene silencing in ES cells.....	41
3.3.1	KLF7 expression analysis following <i>Oct4</i> and <i>Nanog</i> gene silencing.....	42
3.4	KLF7 role in mesenchymal differentiation.....	43
3.5	KLF7 role in NSC.....	45
3.6	KLF7 role in dopaminergic system development.....	49

### **CHAPTER 4 – DISCUSSION .....**

### **BIBLIOGRAPHY.....**

## ABBREVIATIONS INDEX

<b>aa</b>	Amino acid	<b>Mb</b>	Midbrain
<b>AADC/DDC</b>	L-aromatic amino acid decarboxylase	<b>MEF</b>	Mouse embryonic fibroblasts
<b>BLBP</b>	Brain lipid-binding protein	<b>MHJ</b>	Mid-hindbrain junction
<b>Bp</b>	Base pairs	<b>MSC</b>	Mesenchymal stem cells
<b>CA</b>	Catecholamine/Catecholaminergic	<b>NGF</b>	Nerve growth factor
<b>CDK</b>	Cyclin dependent kinase	<b>NGS</b>	Normal goat serum
<b>CNS</b>	Central nervous system	<b>NSC</b>	Neural stem cells
<b>Cys</b>	Cysteine	<b>OB</b>	Olfactory bulbs
<b>DA</b>	Dopamine/dopaminergic	<b>OE</b>	Olfactory epithelium
<b>DAT</b>	Dopamine transporter	<b>P</b>	Postnatal day
<b>DRG</b>	Dorsal root ganglia	<b>PBS</b>	Phosphate buffered saline
<b>E</b>	Embryonic stage	<b>PD</b>	Parkinson's disease
<b>EB</b>	Embryoid body	<b>PNS</b>	Peripheric nervous system
<b>ECM</b>	Extracellular matrix	<b>RMS</b>	Rostral migratory stream
<b>EGFR</b>	Epidermal growth factor receptor	<b>RNAi</b>	RNA interference
<b>ES</b>	Embryonic stem	<b>RrF</b>	Retrosubral field
<b>FGF8</b>	Fibroblast growth factor-8	<b>RT</b>	Room temperature
<b>Fw</b>	Forward	<b>Rv</b>	Reverse
<b>GAPDH</b>	Glyceraldehyde-3-phosphate	<b>SGZ</b>	Subgranular zone
<b>GFAP</b>	Glial fibrillary acidic protein	<b>SHH</b>	Sonic Hedgehog
<b>GZ</b>	Germinal zone	<b>shNS</b>	Short hairpin non silencing
<b>His</b>	Histidine	<b>shRNA</b>	Short hairpin RNA
<b>HPRT</b>	Hypoxanthine phosphoribosyltransferase	<b>SNe</b>	<i>Substantia nigra pars compacta</i>
<b>ISH</b>	<i>In situ</i> hybridization	<b>SVZ</b>	Subventricular zone
<b>KLF</b>	Krüppel-like Factor	<b>TF</b>	Transcription factor
<b>KO</b>	Knockout	<b>TH</b>	Tyrosine hydroxylase
<b>L-DOPA</b>	L-dihydroxy-phenylalanine	<b>VTA</b>	Ventral tegmental area
<b>LIF</b>	Leukemia inhibitory factor	<b>wt</b>	Wild type

**CHAPTER 1**  
**INTRODUCTION**

# 1 INTRODUCTION

## 1.1 Transcription factors.

The regulation of tissue- and development-specific expression of eukaryotic genes is a fundamentally important process that represents the focus of research for numerous molecular biologists. A great deal of attention has been paid to the study of transcription factors (TFs), key elements in the regulation of gene expression that interact with *cis*-regulatory DNA elements in specific genes. Most TFs are classified on the basis of structural motifs that they use to bind to DNA (Yang 1998).

## 1.2 The zinc finger transcription factors family.

The zinc finger motif is an important example of DNA-binding sequence. As the name implies, a zinc finger is a finger-shaped fold in a protein that allows it to bind to its target. It contains a single zinc atom, which serves as a critical structural component of the finger motif. Proteins with zinc finger motifs fall into several groups, according to the three-dimensional appearance of their DNA-binding domain and the amino acids that coordinate the  $Zn^{2+}$ -ion. The Cys<sub>2</sub>-His-Cys motif is exemplified by the myelin transcription factor I MyTI (Kim et Hudson 1992). A second motif that chelates zinc ions with a cluster of 6 cysteines (Cys<sub>6</sub>) characterizes GAL4, a positive regulator of galactose metabolism in *Saccharomyces cerevisiae* (Keegan et al. 1986). The Cys<sub>2</sub>-Cys<sub>2</sub> and the Cys<sub>2</sub>-His<sub>2</sub> zinc fingers tetrahedrally coordinate a zinc atom within a 30 amino acids sequence to form the DNA-binding domain with either 4 cysteines (Cys<sub>2</sub>-Cys<sub>2</sub>

type) or 2 cysteins and 2 histidines (Cys<sub>2</sub>-His<sub>2</sub> type). They also share the property of contacting the major groove of DNA with an  $\alpha$ -helix. The transcription factor GATA-1 is an example of the Cys<sub>2</sub>-Cys<sub>2</sub> motif and is found at all stages of erythroid development in vertebrates (Hannon et al. 1991).

The Cys<sub>2</sub>-His<sub>2</sub> type of zinc finger motif is characterized by a three-dimensional structure made up of two antiparallel  $\beta$ -sheets and an  $\alpha$ -helix (Berg 1988), called the “recognition helix”, that contacts 3 base pairs (bp) of DNA (Berg and Shi 1996) via 3 amino acids. The *Xenopus laevis* transcription factor TFIIIA was the first Cys<sub>2</sub>-His<sub>2</sub> zinc finger protein identified (Pelham and Brown, 1980). In the completely sequenced *Caenorhabditis elegans* genome, 138 proteins (0.7% of all proteins) contain the Cys<sub>2</sub>-His<sub>2</sub> motif (Clarke and Berg, 1998). In comparison, there are 352 (2.6%) Cys<sub>2</sub>-His<sub>2</sub> zinc finger proteins in the genome of *Drosophila melanogaster* (Adams et al., 2000). It has been estimated that: 1% of the human genome consists of genes encoding Cys<sub>2</sub>-His<sub>2</sub> type of zinc finger protein (Hoovers et al., 1992). This would correspond to between 700 and 1000 genes encoding distinct zinc finger proteins (Klug and Schwabe, 1995).

Commonly, this type of motif is found in repeats, and consequently, fingers with different DNA triplet preferences combine to create greater specificity in recognizing longer DNA stretches (Klug 1999).

### **1.3 The Krüppel-Like transcription factors.**

A subfamily of the Cys<sub>2</sub>-His<sub>2</sub> -zinc fingers has been named Krüppel-like factors (KLFs) based on homology to the *Drosophila* segmentation gene Krüppel (Preiss et al. 1985, Bieker 2001). They possess 3 C-terminal Zinc-fingers spaced by the highly conserved HC-link, TGEKPYX (X representing any amino acid), first identified in *Drosophila* (Klug et Schwabe 1995). Additionally, the zinc fingers contain the CX<sub>2-5</sub>CX<sub>3</sub>F/YX<sub>3</sub>LX<sub>2</sub>HX<sub>3</sub>H (where X is any amino acid)-consensus sequence that is also found in TFIIIA (Miller et al. 1985), as well as in members of the Sp1 (Kadonaga et al. 1987; Hagen et al. 1992) and early growth response proteins (Madden and Rauscher 1993).

The Krüppel protein is aptly named because *Drosophila* embryos homozygous for this protein have altered anterior abdominal and thoracic segments, resulting in death (Nusslein-Volhard et al., 1980, Preiss et al., 1985). The first mammalian Krüppel, erythroid Krüppel-like factor (EKLF/KLF1), was identified in red blood cells (Miller et Bieker 1993). This factor was subsequently found to play an important role in  $\beta$ -globin gene synthesis and erythrocyte development (Perkins et al., 1995, Nuez et al., 1995). Since the initial discovery of EKLF in 1993, a total of 17 mammalian Krüppel have been identified and designated based on the chronological order of discovery (i.e., KLF1 to -17). All members of the KLF family are able to bind to similar DNA sequences, such as the “CACCC” sequence or the “GT box”. Indeed as mentioned above, there are three amino acids in each zinc finger that contact base-triplets of DNA thus specifying the binding. Therefore proteins with conserved amino acids in that region will most likely have the same or at least very similar target sequences. Although the zinc finger domains are very similar, the non-DNA-binding domains are highly divergent. Transcriptional regulation by KLFs is mediated via their identified modular activation and repression domains. The zinc fingers of a few family members are aligned in figure 1 to show the conservation of DNA-contacting amino acids which results in common or very similar target sequences. Among all the KLFs, structural and functional considerations have segregated KLF6 and KLF7 into a phylogenetically distinct group (Matsumoto et al., 1998).



**Figure 1: Amino acid sequence alignment of the zinc finger region of some KLFs.**

Residues conserved among all members are shown in green. The cysteine and histidine residues involved in the coordination of zinc are shown in red. The amino acids thought to contact DNA are indicated in yellow.

Figure 2 shows binding sites of some Krüppel-like factors and the conserved amino acids that make contact with base triplets.

KLF1	5'	A	G	G		G	T	G		T	G	G	3'
KLF4	5'	A	G	G		G	C	G		T	A	G	3'
KLF5	5'	G	G	G		G	C	G		G	G	G	3'
KLF6	5'	T	G	G		G	T	G		G	G	G	3'
KLF7	5'	N	G	G		G	N	G		N	G	G	3'

### KLF7 CONSENSUS BINDING MOTIF:



**Figure 2: Binding motifs for selected KLFs**

Residues conserved among all members are shown in green. KLF7 consensus motif is given below along with the amino acid sequence of the zinc fingers showing in yellow the critical residues that directly contact DNA.

## 1.4 The Krüppel-Like Factor 7.

KLF7 was originally identified by RT-PCR performed on RNA from vascular endothelial and rat chondrosarcoma cells using degenerate primers that correspond to regions in the DNA-binding domain of KLF1 (Matsumoto et al., 1998). The human (h) and mouse (m) KLF7 proteins are virtually identical and theoretically code for 33-kD protein of 302 amino acid (aa). It consists of a 76 aa acidic N-terminus, a 136 aa hydrophobic middle segment rich in serines, and a 90 aa C-terminus with the conserved three zinc fingers (fig. 3). Additional features

include a nuclear localization signal (NLS) KKRVHR (aa 215-220), a potential phosphorylation site by ERK kinases in the hydrophobic segment and an *in vitro* binding to the consensus sequence 5' GGNGNGGGN 3' (Matsumoto et al., 1998). Moreover Matsumoto et al., showed by CAT assay that the transcriptional activation property lies within the amino-terminal region, and, by FISH analysis, that the *hKlf7* gene maps to chromosome 2q33.3, a segment of conserved synteny with mouse chromosome 1, C2, where the *mKlf7* gene is located.

It has been identified also a *Drosophila* KLF7 orthologue. Indeed a database search with the conserved region of the mammalian KLF6/KLF7 group yielded the identification of the *Drosophila* gene *Luna*. Its DNA-binding domain bears 97% similarity to the mammalian KLF7 and additionally, high levels of sequence homology were found in 47 aa of the acidic domain, the nuclear localization signal and the putative protein interaction/ ERK consensus sequence (De Graeve et al., 2003).

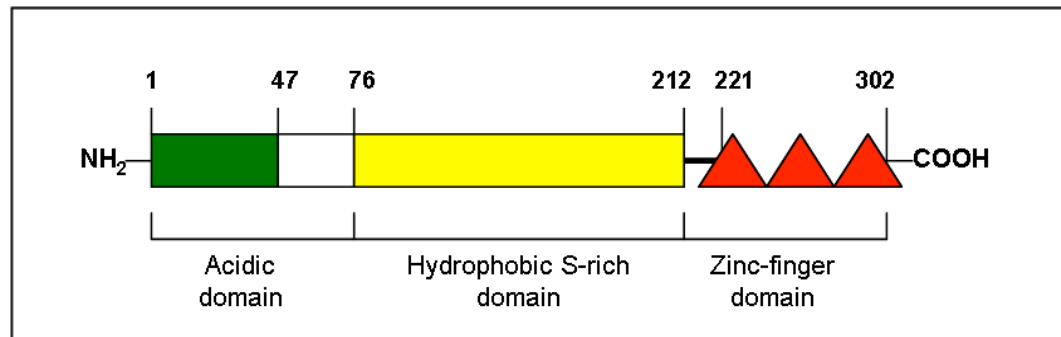


**Figure 3: Schematic view of the KLF7 protein**  
Amino acids references at the points of transition are indicated with numbers.

### 1.4.1 The Krüppel-Like Factor 7 expression.

Preliminary northern analysis on human newborn tissues showed the ubiquitous expression of hKLF7, indeed it was originally called UKLF, for ubiquitously expressed KLF (Matsumoto et al., 1998). Further analysis on mouse tissues showed that, during development, *Klf7* expression is predominantly confined to the nervous system and that it can be divided into three distinct phases (Laub et al., 2001).

In the embryonic phase *Klf7* mRNA appears at about embryonic stage (E) 9,5 both in the central nervous system (CNS) and in the peripheric nervous system (PNS), is maximal at about E11,5 and declines later. By E11,5 *Klf7* is intensively expressed in the forebrain, midbrain, hindbrain, the neural tube, the trigeminal, superior cervical and dorsal root ganglia (DRG). It is remarkable the strong *Klf7* expression in the ventral midbrain (Mb) where the important contingents of dopaminergic neurons reside; as I will explain later, this developmental stage is crucial for dopaminergic neurons development. From E11,5 to E16,5 *Klf7* expression turn from to be predominant in the nervous system to be weak and diffusely distributed throughout the whole embryo (fig. 4a).

*Klf7* postnatal expression is accumulated most strongly in the cerebral cortex and hippocampus, nasal epithelium, trigeminal ganglion and rostral migratory stream (RMS) (fig. 4b). In the adult stage *Klf7* is almost exclusively confined to the cerebellum and DRG, and with lower intensity is still expressed in the olfactory bulbs (OB), hippocampus and some brain-stem nuclei (fig. 4c).

In summary, *Klf7* is not expressed in the proliferative ventricular zone of spinal cord or brain, but only in the developing mantle zone and cortical plate, which contain differentiating postmitotic neuroblasts.

In accordance with the mouse KLF7 expression, analysis of *Luna* by northern blot and *in situ* hybridization (ISH) showed that its expression in the *Drosophila* embryo peaks between stages 6 and 15 and is strictly confined to the nervous system of the fully developed embryo (De Graeve et al., 2003).

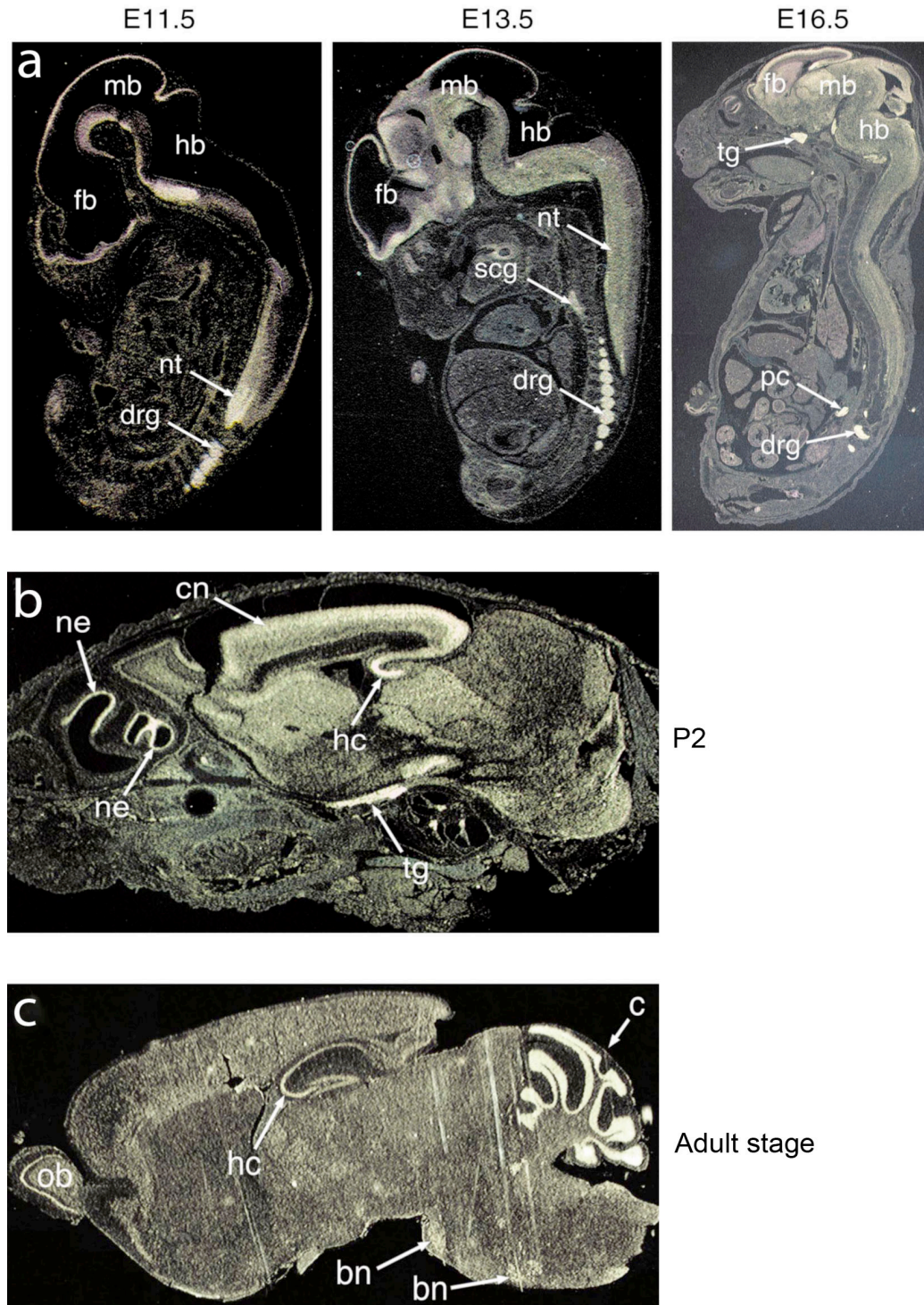


**Figure 4: Temporal profile of *Klf7* expression.**

*Klf7* ISH analysis on sagittal sections, during embryonic development (a), at P2 (b) and at adult stage (c). Abbreviations: fb, forebrain; mb, midbrain; hb, hindbrain; nt, neural tube; drg, dorsal root ganglia; scg, superior cervical ganglia; tg, trigeminal ganglia; pc, plexus coeliacus; ne, nasal epithelium; cn, cerebral cortex; hc, hippocampus; ob, olfactory bulb; c, cerebellum; bn, brain stem nuclei (Laub et al., 2001).

## 1.4.2 The Krüppel-Like Factor 7 functional role.

### 1.4.2.1 KLF7 molecular function.

Using Tet-on/Tet-off inducible gene system Ramirez and coworkers showed that KLF7 overexpression in cultured fibroblasts, results in decreased DNA-replication and, at the same time, increase in the expression of the cyclin dependent kinase (CDK) inhibitor  $p21^{waf/cip}$  (Laub et al., 2001). Consistent with these findings, growth arrest and upregulation of  $p21^{waf/cip}$  were also induced by overexpressing KLF7 through an adenoviral vector in the human neuroblastoma cell line NB-OK-1 (Laub et al., 2001). Further it has been demonstrated that KLF7 directly binds to and stimulates the activity of the proximal promoter of the CDK inhibitor  $p21^{waf/cip}$  and  $p27^{kip1}$  genes (Smaldone et al., 2004; Laub et al., 2005).

These data suggest that KLF7 has an antiproliferative effect and may participate in neuroblast differentiation and cell cycle exit.

### 1.4.2.2 KLF7 biological function.

Most of KLFs are implicated in regulating important developmental programs, such as erythropoiesis, vasculogenesis and lymphopoiesis. KLF7 plays a similar role in the developing nervous system. The functional data about KLF7 role during development derive mainly from the analysis of the *Klf7*-knockout (KO) mouse. Loss of KLF7 activity in mice leads to neonatal lethality, severely affects the development of the olfactory system and perturbs neurite outgrowth and branching throughout the nervous system (Laub et al., 2005).

In the CNS of *Klf7*-KO mice, particularly evident is the olfactory bulbs (OB) hypoplasia, the dendritic impairment in the hippocampus and the axonal misprojections in the cortex (fig. 5).

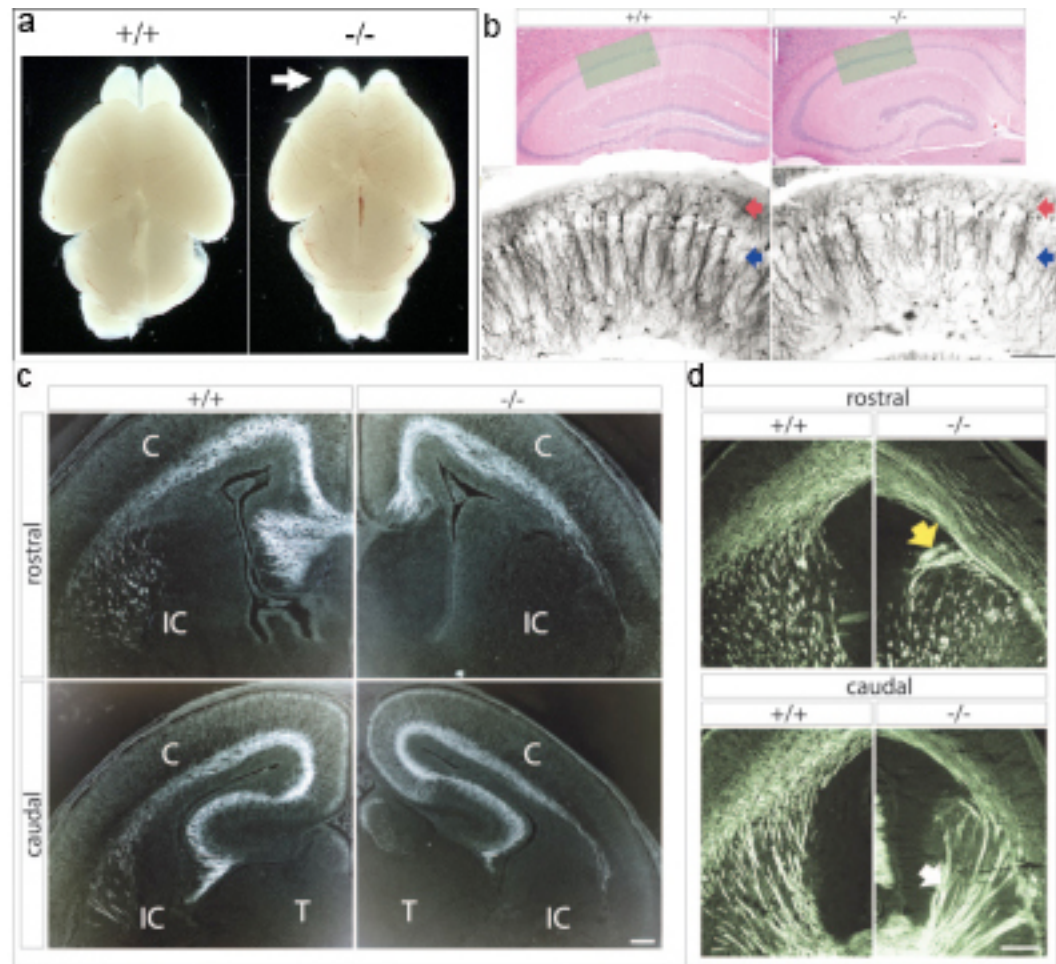


**Figure 5: *Klf7*-KO brain characterization**

a) Lack of fully formed OB in *Klf7*-KO brain (white arrow); b) hematoxylin and eosin staining showing impaired dendritic arborization in *Klf7*-KO hippocampus. In the lower panels is shown a Golgi-Cox staining on pyramidal neurons corresponding to the green shaded areas; c) Sections stained by anti-TAG-1 antibodies to visualize cortical efferent projections at two levels along the rostral-caudal axis; d) sections stained by anti-L1 antibodies to visualize cortical afferent projections at two levels along the rostral-caudal axis. The yellow arrow indicates fiber misprojection, whereas the white arrow highlights axon hyperfasciculation (Laub et al., 2005).

To further investigate about the olfactory system deficit in *Klf7*-KO mice, it has been performed an RNA microarray analysis on wild type (wt) and *Klf7*-KO olfactory epithelium (OE) that revealed alterations of the expression levels of a number of genes involved in synaptic vesicle trafficking and neurotransmission, axon growth, regulation of cytoskeletal dynamics, and cell adhesion. Among the latter, the *L1cam* cell adhesion molecule and the OSN-specific *Omp* showed to be directly activated by KLF7 binding (Kajimura et al., 2006). Thus KLF7 role

during nervous system development seems to be directly involved in cell adhesion and neuronal morphogenesis processes.

In the PNS *Klf7* is coexpressed with *TrkA* in sensory and sympathetic neurons during development and binds specifically to an Ikaros core binding element that is crucial for in vivo *TrkA* enhancer function (Lei et al., 2001). Moreover in *Klf7*-KO mice there is a significant reduction in nociceptive neurons that normally depends on TRKA for NGF neurotrophic support (Lei et al., 2005). These data indicate that KLF7 may directly regulate *TrkA* gene expression during PNS development.

Subsequently it has been suggested that KLF7 may have a broad biological role, not only in the nervous system. Indeed Loh et al. (2006) showed that KLF7 is a potential direct target of stemness master genes such as *Oct4* and *Nanog* in ES cells (Boiani et Scholer, 2005). Moreover KLF7 was found to be potentially implicated in the ES cells self-renewal regulatory pathways (Ivanova et al. 2006). In addition, *Klf7* overexpression leads to a remarkable inhibition of adipogenesis both in mouse 3T3-L1 preadipocytes cells and in human preadipocytes (Kanazawa et al. 2005, Kawamura et al. 2006).

In *Drosophila* it has been shown that *Luna* ectopical overexpression in various tissues at different times during development, resulted in a variety of abnormalities, including inability to fly due to wing malformation or to react to mechanically exerted stimuli, as well as malformation of the eye. These phenotypic consequences of *Luna* misexpression suggest a role in cell differentiation and embryonic development, not unlike those mentioned for its mammalian counterpart (De Graeve et al., 2003).

In summary *Klf7* biological role is tightly linked to developmental processes. Experimental evidence has highlighted a clear role for KLF7 in the nervous system development, but still it is not known if KLF7 is involved in the development of specific populations of CNS neurons. Given its expression in the ventral Mb it is attractive to imagine a KLF7 involvement in dopaminergic neuron development. Moreover *Klf7* expression in the RMS, legitimize the question

about the link between neural stem cells (NSC) and KLF7 function. It is useful to briefly describe these two neural populations.

### **1.5 Neural stem cells.**

NSC are characterized by three cardinal features: (i) they are ‘self-renewing’, with the theoretically unlimited ability to produce progeny indistinguishable from themselves; (ii) they are proliferative, continuing to undergo mitosis (though perhaps with quite long cell cycles); and (iii) they are multipotent for the different neuroectodermal lineages of the CNS, including the multitude of different neuronal and glial subtypes (McKay R. 1997).

#### **1.5.1 NSC location in the embryonic and adult mammalian CNS.**

In the mammalian embryonic CNS, particularly in the ventral telencephalon during mid-neurogenesis and, to a lesser extent, in the dorsal telencephalon, neuroepithelial cells give rise to radial glia, which differentiate into basal progenitors that each form two postmitotic neurons. Both radial glia and neuroectodermal cells can directly generate neurons (Gotz and Huttner, 2005), and both neuroepithelial cells and radial glia can self-renew while producing basal progenitors, neurons or glia. These self-renewing cell types share a similar epithelial morphology, both express the intermediate filament Nestin and have an apically located mitotic spindle, and both can be distinguished by an array of molecular markers, including brain lipid-binding protein (BLBP), RC2, GLAST, and PAX6 (Gotz 2003; Rakic 2003).

In the adult mammalian brain, neurogenesis constitutively occurs only in the OB and the dentate gyrus of the hippocampus. In the olfactory system, precursor cells reside in the anterior aspect of the subventricular zone (SVZ, sometimes also called the subependymal zone) in the walls of the lateral ventricles, migrate via ‘chain migration’ through a structure surrounding the remnants of the olfactory ventricle (RMS) into the OB, and differentiate into granule or periglomerular

interneurons (Lois & Alvarez-Buylla 1993; Luskin 1993; Goldman 1995; Doetsch et al. 1999). In the dentate gyrus of the hippocampus, the precursor cell population is found in the subgranular zone (SGZ) of the dentate gyrus. Here, new hippocampal granule cell neurons are produced. These two brain regions are thus referred to as ‘neurogenic regions’ of the adult brain.

### **1.5.2 An *in vitro* tool to study NSC: neurospheres.**

Neurospheres are floating structures that can be obtained by exposing dissociated embryonic or adult CNS tissue to growth factors (Reynolds et al., 1992; Reynolds and Weiss, 1992, 1996; Weiss et al., 1996). These heterogeneous spheroid structures contain NSC progenitors and differentiated cells embedded in a complex extracellular matrix (ECM) and organized three dimensionally with a core of differentiating glial fibrillary acidic protein (GFAP)<sup>+</sup> and  $\beta$ -tubulin III<sup>+</sup> cells surrounded by Nestin<sup>+</sup>, epidermal growth factor receptor (EGFR)<sup>+</sup> and  $\beta$ 1 integrin<sup>+</sup> undifferentiated cells (Campos et al., 2004). Neurospheres are useful to evaluate NSC multipotentiality (through the characterization of cell phenotypes that arise from a differentiating sphere) and to analyze NSC self renewal using clonal secondary neurosphere assay that assume isolate true stem cells can generate new spheres.

### **1.6 The dopaminergic system.**

The dopaminergic system is composed by groups of neurons producing the neurotransmitter dopamine (DA). DA is one of the catecholaminergic (CA) neurotransmitters of the vertebrate CNS, where it is synthesized in a common biosynthetic pathway as a precursor to noradrenaline and adrenaline. Tyrosine hydroxylase (TH) is the first and rate-limiting enzyme in this pathway that converts the essential amino acid tyrosine to L-dihydroxy-phenylalanine (L-DOPA). LDOPA is then decarboxylated by the enzyme L-aromatic amino acid decarboxylase (AADC/DDC) to produce dopamine (fig. 6).

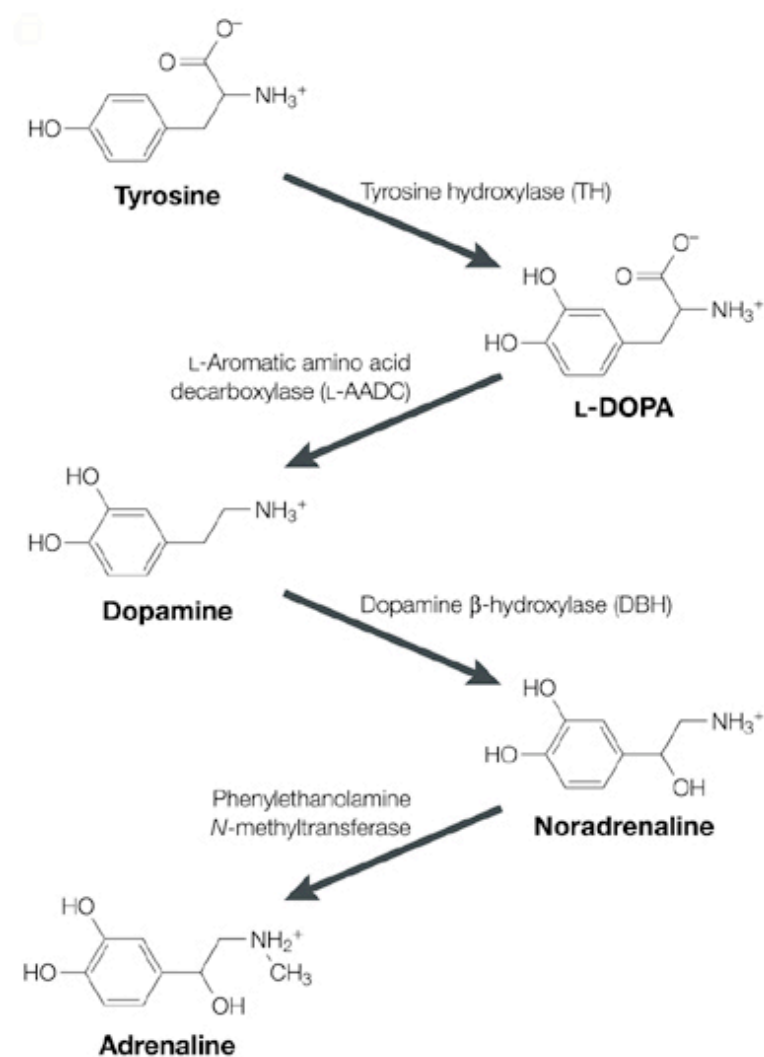


**Figure 6: Dopamine biosynthesis pathway.**

The enzymes mediating each biochemical step are indicated on the arrows.

Expression of *Th* has therefore been widely used as a molecular marker for CA-synthesizing neurons. Much attention has been paid in recent years to the population of DA neurons in the mammalian brain given their pivotal role in the control and modulation of motor and endocrine functions, and affective and cognitive behaviours. The cell bodies of these neurons are found in stereotypic positions within the mammalian brain (Bjorklund and Dunnet, 2007), as listed below from caudal to rostral (fig. 7):

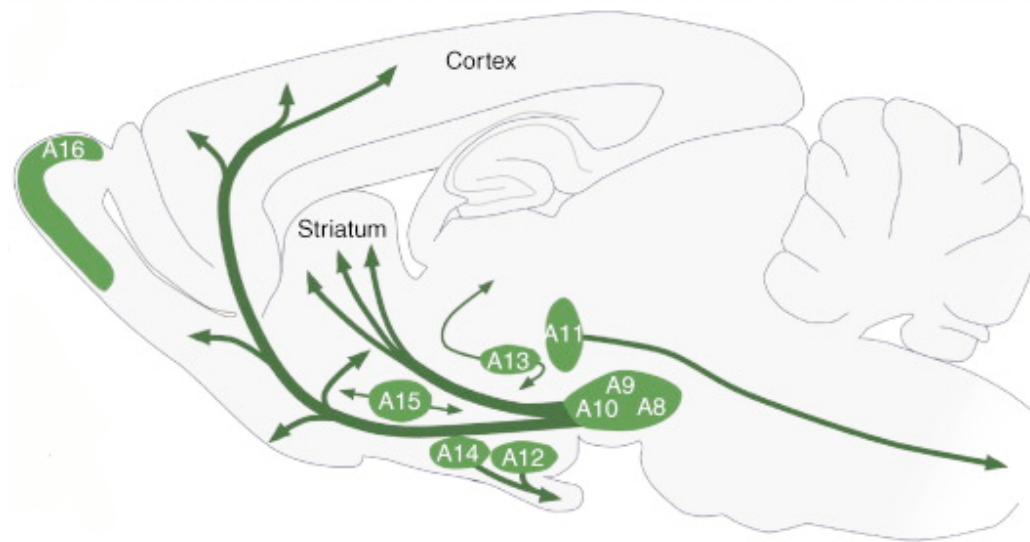


**Figure 7: Distribution of dopaminergic neurons in the adult rodent brain.**

The dopamine neurons in the mammalian brain are localized in nine distinctive cell groups, distributed from the ventral Mb to the OB, as illustrated schematically, in a sagittal view. Arrows illustrate the principal projections of the DA cell groups.

1) DA neurons of the ventral midbrain are arranged in three distinct nuclei: the *substantia nigra pars compacta* (SNc), the ventral tegmental area (VTA); in the retrorubral field (RrF). Historically, these DA cell groups were designated A8 (RrF), A9 (SNc) and A10 (VTA). They represent a small contingent of CNS neurons, from a few thousands in the rodent to a few hundred thousands in human. Cells of the SNc are involved in the control of voluntary movements and postural reflexes, and their degeneration in the adult brain leads to Parkinson's disease (PD), whereas cells of the VTA modulate rewarding and cognitive behaviours, and their dysfunction is involved in the pathogenesis of addictive disorders, depression, attention deficit hyperactivity disorder and schizophrenia.

2) Another population of DA neurons is found in the diencephalon and comprises the A11–A15 groups consisting of approximately 1000 cells. The largest groups are the DA neurons of the posterior hypothalamus (A11) and of the *zona incerta* in the ventral thalamus (A13).

3) Finally, a small DA cell population is found in the telencephalon,

comprising the A16 group of olfactory bulb periglomerular interneurons and the A17 group of retina amacrine interneurons.

### 1.6.1 Development of dopaminergic neurons.

The establishment of functional Mb-DA neurons from multipotent progenitors is orchestrated by cell-intrinsic factors and environmental cues and occurs through a complex multi-step process with a number of stages: early Mb patterning, induction of precursors, differentiation of postmitotic neurons, and functional maturation (Abeliovich and Hammond 2007; Ang 2006). Key regulators of this developmental time course are the activation of TFs and the action of secreted molecules. Their role and subsequent action in the various stages of rodent DA neuron development are summarized in figure 8.

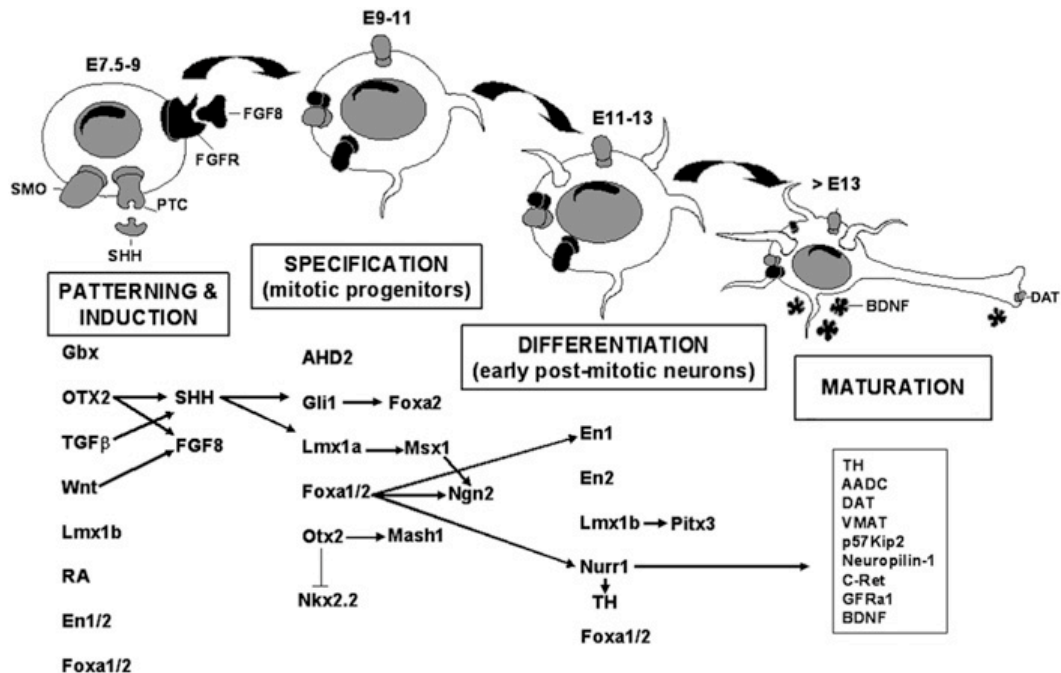


**Figure 8: Diagram model of midbrain dopaminergic neuron development.**

The diagram summarizes the sequential stages and the molecules involved in rodent midbrain DA neuron embryonic development. The expression of TFs and secreted molecules involved in the induction, specification, differentiation and maturation of the Mb-DA phenotype are indicated, at various embryonic (E) ages. Arrows indicate possible interactions between these networks of molecules (Perrone-Capano et al., 2008).

### **1.6.1.1. Early midbrain patterning and induction of DA precursors.**

The specification of the permissive region for DA neuron generation is a fundamental event that initially occurs through the formation and positioning of molecular borders, such as the mid-hindbrain junction (MHJ, also known as *isthmus*). Together with the floor plate, an embryonic structure lining the ventral midline of the neural tube, the MHJ is a key signaling center in the developing Mb. Initially, expression of the two homeodomain TFs, *Otx2* in the Mb and *Gbx2* in the hindbrain, are required for positioning the MHJ, which is a source of inductive molecules required for the specification of the Mb-DA neuronal field. Both *Otx1* and *Otx2* play a remarkable role in specification and regionalization of the forebrain and Mb (Simeone et al. 2002). *Gbx2* regulates Mb and cerebellar development primarily through the secreted fibroblast growth factor-8 (FGF8). The latter, together with the morphogen Sonic hedgehog (SHH), derived from the floor plate of the ventral midline, cooperate in the induction of DA neurons early during gestation (before day E9.5 in mouse).

### **1.6.1.2. Differentiation of postmitotic DA neurons.**

Recent studies indicate that Mb-DA neuroblasts, generated near the MHJ, are derived from the medial floor plate region (Kittappa et al. 2007). As these precursors exit from the cell cycle, they radially migrate from the ventricular surface to their final position in the ventral Mb. Birthdating studies using 3H-thymidine incorporation show that DA progenitors exit the cell cycle and generate postmitotic immature Mb-DA neurons between E9.5 and E13.5 in rodents (Bayer et al. 1995). Immature Mb-DA neurons then further differentiate into mature DA neurons that express TH, in addition to the other markers mentioned above. The first TH+ cells and fibers have been detected close to the ventricular ependymal layer, suggesting that DA differentiation can occur in early radially migrating postmitotic Mb-DA precursors (di Porzio et al. 1990). Several key TFs, such as *Engrailed (En)* 1 and 2, *Nurr1*, *Pitx3* and *Lmx1b* are involved in the development

of postmitotic Mb-DA neurons (fig. 7). However, none of these TFs appears by itself sufficient to specify all aspects of mature Mb-DA phenotype, suggesting that they must act in a combinatorial manner.

### **1.6.1.3. Maturation and survival of the dopaminergic phenotype.**

Following the early commitment of DA neuroblasts, the activation of genes involved in DA neurotransmission takes place in a precise temporal sequence during embryonic development under the control of various environmental cues.

By monitoring the expression of a number of “dopaminergic” genes and their function during embryonic development of the Mb, it has been shown that DA synthesis, storage and high-affinity uptake develop asynchronously (Perrone-Capano and di Porzio 1996, 2000). Following *Th* gene expression, the gene coding for *Vmat-2* is readily expressed. These events take place several days before the establishment of nigrostriatal connections (which in rodents occurs at E15–16). They suggest that VMAT-2 could play a protective role before the establishment of functional DA neurotransmission, since its activity is necessary to accumulate DA into presynaptic vesicles and thus clear it from the cytoplasm. Thus, VMAT-2 limits DA oxidation (since dense core vesicle pH is acidic) and its neurotoxic effects.

Interactions of presynaptic Mb-DA neurons with striatal target neurons play an important role, at least *in vitro*, in promoting key aspects of DA neurotransmission, namely DA synthesis and uptake, mediated by TH and the dopamine transporter (DAT), respectively (Prochiantz et al. 1979; di Porzio et al. 1980; Perrone-Capano and di Porzio 1996).

Interestingly, recent data support the hypothesis that correct target recognition may improve maintenance and survival of DA neurons. It has been proposed that ephrin signaling (involved in axonal guidance) can regulate the correct targeting of nigrostriatal neurons (Yue et al. 1999). Indeed application of ephrin-B2 (expressed *in vivo* by the developing *striatum*) to Mb cultures results in *Nurr1* upregulation (Calò et al. 2005). Other guidance cues can contribute to regulate

correct Mb-DA projections, such as netrin-1 and slit-2, which act in concert to regulate and direct Mb-DA neurites outgrowth (Smidt and Burbach 2007).

### 1.7 Thesis project aim.

During my thesis work I have studied the role of KLF7 both in cellular differentiation and in neuronal morphogenesis. My principal aims were:

- 1) To understand KLF7 involvement in specific differentiation processes like neurogenesis, cardiogenesis, adipogenesis and osteogenesis.
- 2) To analyse KLF7 role during mouse CNS embryogenesis.

In my experimental plan I have used both *in vitro* and *in vivo* approaches to identify KLF7 biological functions.

In the *in vitro* approach I have performed RNA interference (RNAi) experiments in order to analyse the effect of KLF7 depletion in the neuronal cell line PC12, and in embryonic stem (ES) cells differentiation processes. To further understand *Klf7* functions in neuronal differentiation, I have compared self-renewal and neuronal differentiation ability of wt and *Klf7*-KO derived neurospheres. Moreover I have analysed the adipogenic and osteogenic potential of mouse embryonic fibroblasts (MEF) derived from *Klf7*-KO mice.

In the *in vivo* approach I have initially analysed *Klf7* expression during wt mouse brain ontogenesis, thus I have performed a transcriptional analysis of the *Klf7*-KO mouse brain. This analysis suggested that *Klf7*-KO mice share a dopaminergic deficit in the ventral Mb as well as in the OB, therefore I have further confirmed the *Klf7* potential involvement in dopaminergic development, by immunohistochemical experiments.

Altogether my thesis experiments aim to shed light on KLF7 functions during developmental processes. Even if it is known that KLF7 is indispensable for the proper development of the mouse embryo, my effort was aimed at clarifying some of the biological mechanisms involved.

**CHAPTER 2**  
**MATERIALS AND METHODS**

## **2 MATERIALS AND METHODS**

### **2.1 Cell cultures.**

#### **2.1.1 PC12 cells.**

PC12 cells were grown in RPMI medium (Invitrogen, Milan, Italy), with 10% horse serum (HS, Invitrogen), 5% fetal bovine serum (FBS, Invitrogen) and 100U/ml penicillin/streptomycin (Invitrogen). To induce neuronal differentiation cells were previously starved for 24 hr and then NGF (Alexis biochemicals, San Diego, CA, USA) 100 ng/ml was added to the medium. Neurites formation was analysed 7 days after differentiation induction.

#### **2.1.2 ES cells.**

Undifferentiated E14/Tg2a ES cells were grown without feeders onto 0.1% gelatin-coated tissue dishes, in DMEM (Invitrogen) supplemented with 15% FBS (Hyclone, Logan, UT, USA), 0.1 mM  $\beta$ -mercaptoethanol (Sigma-Aldrich, Milan, Italy), 1 mM sodium pyruvate (Invitrogen), 1X non essential aminoacids (Invitrogen), 2 mM glutamine (Invitrogen), 100 U/ml penicillin/streptomycin (Invitrogen) and  $10^3$  U/ml leukemia inhibitory factor (LIF) (Chemicon International, Temecula, CA, USA). ES cells were routinely passaged every 2 days, and the medium was changed on alternated days.

##### **2.1.2.1 ES cells neuronal differentiation.**

$3 \times 10^3$  cells/cm<sup>2</sup> ES cells were plated on 0,1% gelatin coated tissue culture in differentiation medium: Knockout Dulbecco's minimal essential medium

supplemented with 15% Knockout Serum Replacement (both from Invitrogen), 0,1 mM  $\beta$ -mercaptoethanol, 2 mM glutamine, 100 U/mL penicillin/streptomycin. Neurites outgrowth was analysed 8 days after neuronal induction (Kawasaki et al., 2000, Ying et al., 2003, Fico et al., 2008).

### **2.1.2.2 ES cells cardiogenic differentiation.**

20  $\mu$ l drops of ES cells (400 cells/drop) in differentiation medium: [(DMEM (Invitrogen) supplemented with 15% FBS (Hyclone), 0.1 mM  $\beta$ -mercaptoethanol (Sigma-Aldrich), 1 mM sodium pyruvate (Invitrogen), 1X non essential aminoacids (Invitrogen), 2 mM glutamine (Invitrogen), 100U/ml penicillin/streptomycin (Invitrogen)] were placed on the lid of tissue culture dishes filled with phosphate buffered saline (PBS, Euroclone, Milan, Italy), and cultivated in hanging drops for 2 days. Two-day-old embryoid bodies (EBs) were then collected in differentiation medium and transferred into 100-mm bacteriological Petri dishes. After further 3 days of culture, 5 day-old EBs were plated in the same medium onto 0,1% gelatin-coated tissue culture plates. Cardiomyocitic formation was assayed at 8 days in culture (Maltsev et al., 1993).

### **2.1.3 Mouse embryonic fibroblasts (MEF).**

#### **2.1.3.1 MEF preparation.**

E14,5 embryos were took in sterile conditions and placed in PBS. The head and viscera were removed and decapitated embryos were washed in fresh PBS, trying to get rid of as many red blood cells as possible. The decapitated embryos were placed in a dish containing Trypsin/EDTA (Invitrogen), and using curved Iris scissors the tissue were quickly finely minced until it can be taken up in a 10ml pipette. More Trypsin/EDTA was added to the dish and again pipetted up and down with a 5ml pipette. Then, the dishes were placed back in the incubator for 10 more minutes. All the contents of the dish were put in a 50ml conical tube. The

pieces of cellular debris were spun down, and the supernatant was put into a fresh tube for a new wash with MEF medium (DMEM, 10% FBS, 100U/ml penicillin/streptomycin). Thus the suspension was spun down again and the pellet resuspended in MEF medium and placed in a T-150 flask. Cells were let grow overnight in the incubator. After this time, the medium was changed to remove any cellular debris and the flask placed back in the incubator for another 24 hours and then passaged. In order to maintain the primary cells characteristics, in all MEF experiments were used cells passaged no more than six times.

### **2.1.3.2 MEF adipogenic differentiation.**

MEF were allowed to grow to 90-95% confluence and then cultured for two weeks in  $\alpha$ -MEM (Invitrogen) supplemented with 10% FBS, 10% HS, 2 mM L-glutamine, 100 U/ml penicillin/streptomycin,  $10^{-6}$  M dexamethasone (Sigma-Aldrich), 5  $\mu$ g/ml insulin (Sigma-Aldrich), 0.5  $\mu$ M 3-Isobutyl- 1-methylxanthine (IBMX) (Sigma-Aldrich) and 50  $\mu$ M indomethacin (Sigma-Aldrich) changing medium every 3-4 days (Digirolamo et al., 1999).

### **2.1.3.3 Oil red-O staining.**

Cells were washed with PBS and fixed in 10% formaldehyde for 10 minutes. After rinsing with distilled water, they were stained with 0,5% oil red-O working solution prepared by vigorously mixing 3 parts of a stock solution (0,5% Oil red-O in isopropanol) (Sigma-Aldrich) with 2 parts of water for 5 minutes and filtering through a 0,4  $\mu$ m filter. Excess staining was removed by washing twice with PBS. Cells were then counterstained with hematoxylin (Bio-Optica) for 3 minutes and then washed with distilled water (Digirolamo et al., 1999). Dye was extracted by isopropanol incubation for 15 minutes at room temperature (RT). Quantitative assessment was obtained by absorbance of a five-fold dilution of the extracted dye at 540 nm.

#### **2.1.3.4 MEF osteogenic differentiation.**

MEF were allowed to grow to 70-90% confluence and then cultured for 3 weeks in  $\alpha$ -MEM supplemented with 10% FBS, 2 mM L-glutamine, 10 U/ml penicillin - 10  $\mu$ g/ml streptomycin,  $10^{-8}$  M dexamethasone, 0,05 mM ascorbic acid 2-phosphate (Sigma-Aldrich) and 10 mM  $\beta$ -glycerophosphate (Sigma-Aldrich), changing medium every 3-4 days (Phinney et al., 1999).

#### **2.1.3.5 Alizarin red S staining.**

Cells were washed with PBS and fixed in 10% formaldehyde for 1 hour; after rinsing with distilled water, they were incubated with 2% alizarin red S (Sigma-Aldrich) pH 4,1 with gentle shaking for 10 minutes. Excess staining was removed by washing twice with PBS (Digirolamo et al., 1999). Dye was extracted by overnight incubation with 4M guanidine-HCl (Sigma-Aldrich) at RT. Absorbance at 490 nm of a five-fold dilution of the resulting supernatant was used for quantitative mineralization determination.

#### **2.1.4 Neurospheres.**

Under a stereoscope in sterile conditions P0 brains were removed and overlying meninges and blood vessels were discarded. The striatal germinal zone (GZ) was dissected according to the coordinates reported in rodent brain atlas (Sherwood and Timiras, 1970; Kruger et al., 1995). The tissue was transferred to 500  $\mu$ l of DMEM/F12 (Invitrogen) medium and mechanically dissociated into a cell suspension with a fire-polished Pasteur pipette. Thus the cells were counted and cultured in suspension  $2,5 \times 10^5$ /ml with neurospheres medium [DMEM/F12, B27 (Invitrogen), N2 (Invitrogen), bFGF and EGF (both 20ng/ml, Sigma-Aldrich)] in 25cm<sup>2</sup> flasks with no substrate pretreatment. Primary neurospheres were formed after 4-5 days *in vitro*, thus every week were softly spinned down (75g),

mechanically dissociated and the medium was changed. In order to maintain the primary neurospheres characteristics all experiments were performed with cells passaged no more than 10 times.

#### **2.1.4.1 Neurospheres neural differentiation.**

To evaluate neural differentiation potential, neurospheres were dissociated and plated  $5 \times 10^4$  cells/cm<sup>2</sup> on poly-D-lysine (15 µg/ml, Sigma-Aldrich) precoated plates in neurospheres medium. After 6 days in culture, cells were kept for additional 3 days without bFGF and EGF, thus neuronal, astroglial and oligodendroglial differentiation were assessed by immunocytochemical analysis.

#### **2.1.4.2 Neurospheres assay.**

To determine the self-renewal skill of secondary neurospheres, primary neurospheres were mechanically dissociated into single cells with a fire polished Pasteur pipette, and an aliquot was counted and cultured 500 cells/200 µl/well in 96-well plates ultra-low attachment (Corning, Milan Italy) (Reynolds and Weiss, 1996). Thus each week, secondary neurospheres formed in each well were counted and passaged in a new single well. 12 wells for both wt and *Klf7*-KO neurospheres were assayed along 4 weeks.

## **2.2 Cell transfections.**

All cell lines were transfected by lipofection using Lipofectamine 2000 transfection reagent (Invitrogen). All transfections were performed in triplicate samples. Transfected cells were selected with puromycin (Sigma-Aldrich) 2 µg/ml 48 hr after transfection. For each experimental condition three pools of resistant clones were generated and were kept separated in all real time RT-PCR and western blot experiments.

### 2.2.1 RNAi.

To silence *Klf7*, *Oct4* or *Nanog* genes expression I used short hairpin RNA (shRNA) expressing vectors contained in the Expression Arrest<sup>TM</sup> mouse shRNA library (Open Biosystems, Huntsville, AL, USA). In all RNAi experiments a short hairpin non silencing (shNS) vector was used as control.

### 2.3 Animal and dissections.

Timed pregnant wt, *Klf7*-heterozygous (het) mice and postnatal day (P)0 or P10 pups (Charles River Breeding Laboratories, Milan, Italy) were sacrificed in accordance with Society for Neuroscience guidelines and Italian law. The embryonic age (E) was determined by considering the day of insemination (as confirmed by vaginal plug) as day E0. Embryos from day 11,5 to E17,5 of gestation were quickly removed and placed in PBS, without calcium and magnesium, and supplemented with 33 mM glucose. All the tissues both from embryos and pups, were dissected according to the coordinates reported in rodent brain atlas (Sherwood and Timiras, 1970; Kruger et al., 1995) and processed for RNA extraction or cell cultures. All embryos and pups tissues deriving from *Klf7*-het pregnant mice, were processed separately and a tail sample was processed for genotyping.

#### 2.3.1 Mice genotyping.

Tail samples were put in 500 µl of lysis buffer [100 mM Tris-HCl pH8,5, 5 mM EDTA, 0,2% SDS, 200 mM NaCl, 100 mg/ml proteinase K (Roche, Milan, Italy)] overnight at 55°C. Thus DNA was extracted adding 500 µl of chloroform/isoamyl alcohol (24:1) shaking for a few seconds and centrifuging at 13000 g for 15 minutes. The upper aqueous phase was collected and the DNA precipitated adding 1 ml of EtOH and centrifuging at 7000 g for two minutes. Thus the DNA pellet was decanted and washed with 70% EtOH. Finally the DNA was dried and resuspended in 300 µl of distilled water. The genotype was identified by PCR

(Laub et al., 2005) with two pair of primers that amplify, the first exon of *Klf7* wt gene and the PGK-neo cassette that replaces *Klf7* first exon in the mutant mice (table 1).

### 2.3.1.1 PCR analysis.

2 µl of DNA were amplified in a 25 µl of reaction mixture containing AmpliTaq Gold DNA polymerase buffer (Applied Biosystems, Milan, Italy), 0,2 mM dNTPs (Finnzymes OY, Espoo, Finland), 0,4 µM each primer, 1 U AmpliTaq Gold DNAPolymerase (Applied Biosystems). The thermal profile of the amplification consisted of a first denaturing step of 5 minutes at 95 °C, 35 cycles of 30 seconds at 95 °C, 40 seconds at 63 °C and 1 minute at 72°C, followed by a final extension of 10 minutes at 72°C. The wt (250 bp) or mutant (420 bp) amplified products were identified after gel electrophoresis in 1,5% agarose gel.

Target	Sequence (5'-3')	Amplicon length (bp)
<i>Bdnf</i> fw	ACAATGTGACTCCACTGCCG	70
<i>Bdnf</i> rv	CACTCTTCTCACCTGGTGGAACT	
<i>Blbp</i> fw	CCAGCTGGGAGAAGAGTTTGA	70
<i>Blbp</i> rv	CATCCAACCGAACCACAGACT	
<i>Cacna1a</i> fw	TGCTGAACCTTGTTCTGGGTG	70
<i>Cacna1a</i> rv	TCTCCGGTTCTCCACACGTT	
<i>Cacna1b</i> fw	ATGGACTTCGTGGTGGTCCTC	70
<i>Cacna1b</i> rv	CTCAGTGTGCGCAGGTCAA	
<i>Dat</i> fw	TCTGGGTATCGACAGTGCCA	70
<i>Dat</i> rv	GCAGCTGGAACATCGACAA	
<i>Dbh</i> fw	GACCGGCTACTGCACAGACAA	70
<i>Dbh</i> rv	GAGAGCAAAGATGTGGATTCC	
<i>Dlx2</i> fw	GTCAACAACGAGCCGGACA	70
<i>Dlx2</i> rv	ACTTTCTTTGGCTTCCCGTTC	
<i>Dlx5</i> fw	CTACAACCGCGTCCCGAG	70
<i>Dlx5</i> rv	TCACCATCCTCACCTCTGGC	
<i>Drd1</i> fw	CTGGCACAAGGCAAACCTAC	70
<i>Drd1</i> rv	TGTCATCCTCGGCATCTTCC	
<i>Drd2</i> fw	GCACAGCAAGCATCTTGAACC	70
<i>Drd2</i> rv	CAACATAGGCATGGCCACAG	
<i>Drd3</i> fw	TCCTCACTAGACAGAACAGCC	70
<i>Drd3</i> rv	CCGCAGACAGGAAGACTGCT	
<i>Drd4</i> fw	AAGGGAGCGCAAGGCAAT	70
<i>Drd4</i> rv	AGAAAGGCGTCCAACACACC	

<b>Target</b>	<b>Sequence (5'-3')</b>	<b>Amplicon length (bp)</b>
<i>Drd5</i> fw	GAGACACCCTGGGAGGAAGG	70
<i>Drd5</i> rv	GTTCGGTTCAGGCTGGAGTC	
<i>Eaat1</i> fw	CCTTCGTTCTGCTCACGGTC	70
<i>Eaat1</i> rv	TTATACGGTTCGGAGGGCAA	
<i>En1</i> fw	CGCCTGGGTCTACTGCACA	70
<i>En1</i> rv	TCTTCTTTAGCTTCCTGGTGCG	
<i>En2</i> fw	GACCGCCTTCTTCAGGTC	70
<i>En2</i> rv	GGCCGCTTGTCTCTTTGT	
<i>Foxa1</i> fw	GAAGGGCATGAGAGCAACGA	70
<i>Foxa1</i> rv	ACAGGGACAGAGGAGTAGGCC	
<i>Foxa2</i> fw	ACGAGCCATCCGACTGGAG	70
<i>Foxa2</i> rv	GGCGTTCATGTTGCTCACG	
<i>Gabat</i> fw	CAATGTGGCCCGTGTGG	70
<i>Gabat</i> rv	TGAACTGAGGGTACTGGGCCT	
<i>Gad1</i> fw	TGCCAAACAAAAGGGCTATGT	70
<i>Gad1</i> rv	CGAATGCTCCGTAAACAGTCG	
<i>Gad2</i> fw	AGGGTACTGATGTCCCGGAA	70
<i>Gad2</i> rv	TCCATGTCACAGAGTTGGC	
<i>Gapdh</i> fw	GTATGACTCCACTCACGGCAAA	70
<i>Gapdh</i> rv	TTCCCATTCTCGGCCTTG	
<i>Gat1</i> fw	GCTGATGCTGGGCATTGAC	70
<i>Gat1</i> rv	GGTACTCGTCCACCAGGGC	
<i>Gat2</i> fw	TCTTCATCATGCTCCTGTTTCTAGG	70
<i>Gat2</i> rv	GGAAGCGGTCACCAGGC	
<i>Gat3</i> fw	GTGACCTCCGAGAATGCCA	70
<i>Gat3</i> rv	CCATCCGAGAGCTTCAGGACT	
<i>Gat4</i> fw	CACCTTGTTCTTCATGATGCTCA	70
<i>Gat4</i> rv	TCACAAGACTCTCCACGCACAC	
<i>Gdnf</i> fw	AGGTCCGGATGGGTCTCCT	70
<i>Gdnf</i> rv	TCTCCGTAGACCCCCAGTTG	
<i>Hprt</i> fw	TGCCCTTGACTATAATGAGTACTTCAG	70
<i>Hprt</i> rv	TTGGCTTTTCCAGTTTCACTAATG	
<i>Klf7</i> fw	CACTTAAAGGCCACCAGAGG	70
<i>Klf7</i> rv	CACTCGCATCCTTCCCATG	
<i>Klf7</i> exon 1 fw	TTTCTGGCAGTCATCTGCAC	250
<i>Klf7</i> exon 1 rv	GGGTCTGTTTGTGTTGTCAGTCTGTC	
<i>Lmx1a</i> fw	AACCAGCGAGCCAAGATGAA	70
<i>Lmx1a</i> rv	TGGGTGTTCTGTTGGTCCTGT	
<i>Lmx1b</i> fw	ACACAGCAGCGAAGAGCTTTC	70
<i>Lmx1b</i> rv	GTCTCTCGGACCTTCCGACA	
<i>Map2</i> fw	AACGGGATCAACGGAGAGCT	70
<i>Map2</i> rv	TGTGACTACTTGAACATCCTTGCAGAT	
<i>Mash1</i> fw	GGGAATGGACTTTGGAAGCA	70
<i>Mash1</i> rv	ATTGACGTCGTTGGCGAG	
<i>Mecp2</i> fw	GGATTCCATGGTAGCTGGGA	70
<i>Mecp2</i> rv	TGAGGCCCTGGAGATCCTG	
<i>Msx1</i> fw	CTCCCCGCCCCAGCCAGAC	70
<i>Msx1</i> rv	GGGCTTGCGGTTGGTCTTGT	

Target	Sequence (5'-3')	Amplicon length (bp)
<i>Nanog</i> fw	TGCTACTGAGATGCTCTGCACAG	70
<i>Nanog</i> rv	TGCCTTGAAGAGGCAGGTCT	
<i>Neurod</i> fw	TGAGATCGTCACTATTTCAGAACCTTT	70
<i>Neurod</i> rv	CGCTCTCGCTGTATGATTTGG	
<i>Ngn1</i> fw	CCAGTAGTCCCTCGGCTTCA	70
<i>Ngn1</i> rv	CAGGCCAGGAAAGGAGAAAAG	
<i>Ngn2</i> fw	ATCTGGAGCCGCGTAGGAT	70
<i>Ngn2</i> rv	CATCAGTACCTCCTCTTCTCCTTC	
<i>Nurr1</i> fw	GTGCCTAGCTGTTGGGATGG	70
<i>Nurr1</i> rv	GTAAACGACCTCTCCGGCC	
<i>Oct4</i> fw	AACCAACTCCCAGGAGTCC	70
<i>Oct4</i> rv	CAGCAGCTTGGCAAACCTGTTT	
<i>Otx2</i> fw	TAACGTCCAATGCGGCTGTA	70
<i>Otx2</i> rv	GGAGTGGACAGGGTCAGGGT	
<i>p21</i> fw	CCACAGCGATATCCAGACATTC	70
<i>p21</i> rv	GCGGAACAGGTCGGACAT	
PGK- <i>neo</i> fw	CCCCTTCGCGCCACCTTCTACTCCTC	420
PGK- <i>neo</i> rv	TGAGCCCAGAAAGCGAAGGAGCAAAG	
<i>Phoxa2</i> fw	AAGATCGACCTCACTGAGGCTC	70
<i>Phoxa2</i> rv	TCCTGTTTGCGGAACCTTGG	
<i>Pitx3</i> fw	GACGCAGGCACTCCACACC	70
<i>Pitx3</i> rv	TTCTCCGAGTCACTGTGCTC	
<i>Ret</i> fw	TGAACCTACCCAGGGCCTACT	70
<i>Ret</i> rv	GACTTTCCCGATCTGGGCAT	
<i>RhoA</i> fw	AGAAGGACCTTCGGAATGACG	70
<i>RhoA</i> rv	AGGTTTTACCGGCTCCTGCT	
<i>Sert</i> fw	GGAACGAAGACGTGTCCGAG	70
<i>Sert</i> rv	TGCCTCCGCATATGTGATGA	
<i>Th</i> fw	CTCACCTATGCACTCACCCGA	70
<i>Th</i> rv	GGTCAGCCAACATGGGTACG	
<i>Tph1</i> fw	ACAACATCCCAGCAACTGGAG	70
<i>Tph1</i> rv	CACAGGACGGATGGAAAACC	
<i>Tph2</i> fw	GACCACCATTGTGACCCTGAA	70
<i>Tph2</i> rv	ACGGCACATCCTCGAGATCT	
<i>TrkA</i> fw	TCGTGGCTGTCAAGGCACT	70
<i>TrkA</i> rv	CAGCTCGGCCTCACGCT	
<i>Uncx4.1</i> fw	TCCCAGAGTTCAGGTCTGGTT	70
<i>Uncx4.1</i> rv	GGGCCCTTTTTGGTGTCTC	
<i>Vgat</i> fw	AGCGGGCTGGAACGTGA	70
<i>Vgat</i> rv	CGTGGAGGATGGCGTAGG	
<i>Vmat2</i> fw	TTGCTCATCTGTGGCTGGG	70
<i>Vmat2</i> rv	TGGCGTTACCCCTCTCTTCAT	

**Table 1: List of primers used for PCR and real time RT-PCR analyses.**

The table shows the forward (fw) and reverse (rv) primers sequence with length of amplified fragments used in PCR and real time RT-PCR experiments.

## 2.4 RNA isolation and real-time RT-PCR analysis.

Total RNA was extracted from cell cultures or tissue samples using the Tri-Reagent isolation system (Sigma-Aldrich) according to the manufacturer's instructions (Chomczynski and Sacchi, 1987). Tissue samples were previously triturated using a plastic coated grinder. The analyses were always carried in triplicate obtained from different pools of samples for each experimental condition and were processed separately. The yield and the integrity of RNA were determined by spectrophotometrical measurement of A260 and agarose gel electrophoresis, respectively. RNA was treated with DNA free kit (Ambion Inc., Milan, Italy) to eliminate possible DNA contaminations. Two  $\mu\text{g}$  of RNA were reverse transcribed using random hexanucleotides as primers (New England Biolabs Inc., Milan, Italy, 6  $\mu\text{M}$ ) and 200 U of moloney-murine leukemia virus reverse transcriptase (Ambion). Real time RT-PCR was carried out using the 7900HT Fast Real-Time PCR System (Applied Biosystems). 1/50 of the reverse transcribed cDNA was amplified in a 25  $\mu\text{l}$  reaction mixture containing 1X SYBR Green PCR Master Mix (Applied Biosystems), and 0,4  $\mu\text{M}$  each primer. The thermal profile consisted of 2 minutes at 50 °C, 10 minutes at 95 °C, followed by 40 cycles of 15 seconds at 95 °C and 1 minute at 60 °C. Gene expression was normalized with *Glyceraldehyde-3-phosphate dehydrogenase (Gapdh)* expression level in PC12 and ES cells experiments and with *Hypoxanthine phosphoribosyltransferase (Hprt)* [which is constantly expressed during CNS development (Steel et Buckley 1993)] in brain tissues analyses. All primers used for the real time RT-PCR experiments were designed with Primer Express 3.0 software (Applied Biosystems) and are listed in table 1.

## 2.5 Western blot analysis.

For western blots analyses, cultures samples were lysed in a buffer 150 mM NaCl, 10 mM Tris-HCl pH8, 0,4 mM EDTA, 1% Triton X-100, containing a cocktail of protease inhibitors (Roche, Milan, Italy). Protein content of each sample was determined by the Bio-Rad assay kit (Bio-Rad laboratories S.r.l., Milan, Italy). 50

µg/lane of proteins were separated on 12% SDS-polyacrylamide gel. Proteins were transferred to PVDF filters (Amersham biosciences, Milan, Italy) in transfer buffer (25mM Trizma, 193 mM glycine, 20% methanol). Filters were soaked for 30 minutes in transfer buffer and were blot for two hours in blocking buffer (10mM Tris-HCl pH 8, 150 mM NaCl, 5% non fat dry milk). Membranes were probed for two hours at RT with anti-KLF7 (Abnova, Taipei, Taiwan, 1:5000), anti-BLBP (1:1000 custom made) or anti-β-ACTIN (1:5000 Santacruz Biotechnology Inc., Santacruz, CA, USA) antibodies in blocking buffer. After washing (four times for 5 minutes each) with TTBS (Tris-HCl 10 mM pH 8,0; NaCl 200 mM, Tween-20 0,1%) and once with TBS (Tris-HCl 10 mM pH 8,0; NaCl 200 mM), immunoblots were incubated with horse radish peroxidase conjugated anti-mouse IgG antibodies (1:10000, Amersham Biosciences) in blocking buffer for one hour at RT and washed as above. The reaction was detected with ECL plus procedure (Amersham Biosciences).

## **2.6 Immunocytochemical analysis.**

Cell cultures were fixed for 30 minutes at RT in 4% paraformaldehyde in PBS, permeabilized for 15 minutes at RT in PBS containing 0,1% Triton X-100 and 10% normal goat serum (NGS), and incubated for 2 hours at RT in PBS containing 10% NGS and primary antibody [anti-βTUBB3 1:1000 (Promega, Madison, WI), anti-GFAP 1:400 (Sigma-Aldrich), anti-NG2 1:400 (Chemicon), anti-BLBP 1:500, anti-Ki67 1:300 (BD Pharmigen), anti-PhosphoH3 1:500 (Cell Signaling Technology, Inc., Danvers, MA, USA), anti-Nestin 1:40 (Developmental Studies Hybridoma Bank, Iowa City, IA, USA)]. The antigens were revealed with incubation for one hour at RT in PBS containing 10% NGS and anti-mouse or anti-rabbit secondary fluoresceine or rhodamine conjugated antibodies (1:400, Chemicon). Nuclei were marked with the nuclear dye DAPI (Roche) and the slides were mounted with Vectashield (Vector Laboratories, Burlingame, CA, USA). Cells counting was performed on five fields from three replicates for each condition and normalized with DAPI positive cells.

## **2.7 Immunohistochemical analysis.**

P0 brains were fixed overnight at 4°C with 4% paraformaldehyde, buffered in 30% sucrose until they sunk, to cryopreserve the tissue, and included in OCT. Frozen brains were cut in 15µm thick sections with a cryostat and processed for immunostaining. Thus frozen sections were permeabilized for 1 hour at RT in PBS containing 0,1% Triton X-100 and 10% normal NGS, and incubated for 2 hours at RT in PBS containing 10% NGS and anti-TH antibody (1:200, Chemicon). The immunoreactive signal was revealed according to standard avidin-biotin immunocytochemistry procedures (Vectastain Elite), using a peroxidase substrate kit (DiAminoBenzidine).

**CHAPTER 3**  
**RESULTS**

### 3 RESULTS

#### 3.1 Expression profile of *Klf7* in proliferating and differentiated PC12 and ES cells.

In order to test KLF7 relevance in cell differentiation pathways, I have first analyzed in two different cellular systems, its transcriptional modulation following differentiation. First I used the rat pheochromocytoma cell line PC12. PC12 cells are useful to study KLF7 functions, since KLF7 activates the transcription of the nerve growth factor (NGF) high affinity receptor *TrkA* (Lei et al., 2005), that in turn mediates PC12 neuronal differentiation following NGF administration. The other cellular system that I have used is the totipotent mouse ES cell line E14 tg2a. The use of ES cells is useful to comprehend the KLF7 potential functions in the development of both ectodermal and mesodermal embryonic cell lineages, since they can be differentiated into neurons or cardiomyocytes.

I have induced PC12 cells neuronal differentiation with NGF, then collected cells after 7 days *in vitro* and performed real time RT-PCR analysis on proliferating and differentiated cDNA samples. This experiment showed a significant increase in *Klf7* transcripts. At the same time I have found a similar increase of *p21<sup>wf/cip</sup>* transcript, as expected since *p21<sup>wf/cip</sup>* is one of the few known KLF7 effectors (Laub et al., 2001)(fig. 1).

ES cells were induced to differentiate into neurons by serum withdrawal, or, alternatively, into cardiomyocytes following EBs formation. In accordance with PC12 experiments, both neuron and cardiomyocyte differentiated cells shared a significant increase in *Klf7* transcript and *p21<sup>wf/cip</sup>* transcript levels in differentiated samples (fig. 9).

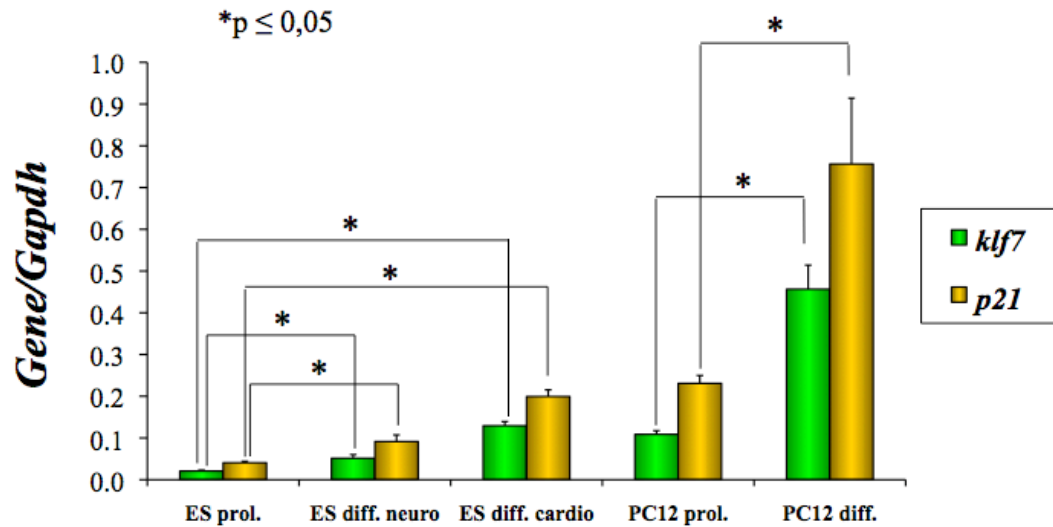


**Figure 9: *Klf7* and *p21* transcriptional changes in ES and PC12 cells following differentiation.**

The diagram shows the relative quantization (mean  $\pm$  SE) of the *Klf7* and *p21* transcripts amplified product compared to that of the glyceraldehyde-3-phosphate dehydrogenase (*Gapdh*, internal standard). Data are expressed as ratio *Klf7/Gapdh* and *p21/Gapdh*. Asterisks represent  $p < 0.05$  when compared to the indicated control cultures (ANOVA, Scheffè F-test).

### 3.2 *Klf7* gene silencing in PC12 cells.

In order to investigate KLF7 function in cellular differentiation, I have performed experiments to silence *Klf7* expression by RNAi. To this aim, I have used a short hairpin RNA (shRNA) expressing vector contained in a shRNA library. The sh*Klf7* construct was designed to specifically silence mouse *Klf7* mRNA. In all RNAi experiments control samples were treated with a non-silencing RNA (shNS) expressing vector.

In order to understand the role of *Klf7* in neuronal differentiation, I have modulated its expression in PC12 cells by stable transfection of the sh*Klf7* or shNS vectors. Thus following puromycin selection I have obtained three pools of transfected clones for each construct. The different pools were kept separated in all the subsequent experiments. Samples of proliferating shNS-PC12 and sh*Klf7*-PC12 cells have been assayed by real time RT-PCR for *Klf7* mRNA levels, showing no differences when compared to controls, consistently with the Open Biosystems shRNA library properties, designed to silence gene function at the protein level. Therefore KLF7 protein level has been assayed by western blots in

shNS-PC12 and sh*Klf7*-PC12 cells. The result has shown a significant decrease of anti-KLF7 immunoreactive signal in sh*Klf7*-PC12 samples compared to control shNS-PC12 clones (fig. 10). In these clones I have found a dramatic decrease of *Klf7* transcripts (fig. 10), associated to a significant reduction of KLF7 protein, as showed for PC12 cells transiently transfected. Moreover real time RT-PCR analysis has shown that in sh*Klf7*-PC12 stable clones, *Map2* mRNA decreased synergistically with *Klf7* mRNA (fig. 10). Finally to investigate whether KLF7 protein depletion in PC12 cells could lead to a transcriptional change in genes involved in PC12 neuronal differentiation, I have analysed the mRNA levels of the NGF receptor *TrkA* in sh*Klf7*-PC12 stable clones and found a significant reduction of its transcripts (fig. 10).

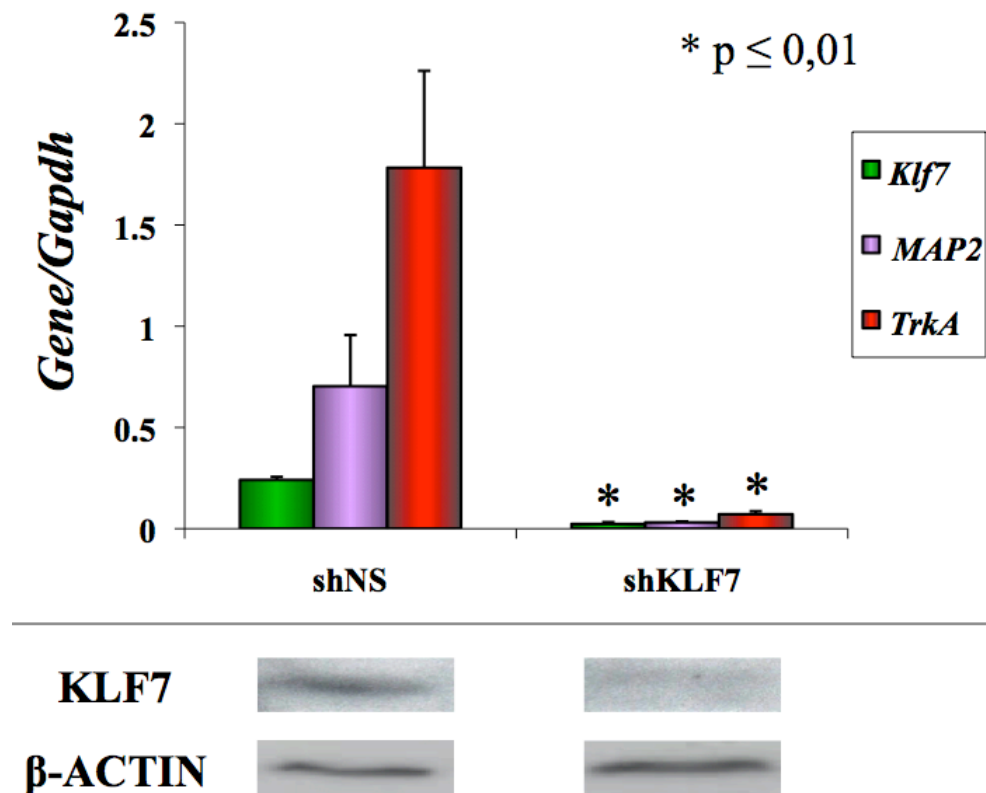


**Figure 10: Transcriptional analysis following *Klf7* stable silencing in PC12 cells.**

The diagrams shows the relative quantization (mean  $\pm$  SE) of the *Klf7*, *Map2* and *TrkA* transcripts amplified product compared to that of the glyceraldehyde-3-phosphate dehydrogenase (*Gapdh*, internal standard). Data are expressed as ratio *Klf7/Gapdh*, *Map2/Gapdh* or *TrkA/Gapdh*. Analyses were performed in PC12 cells transiently transfected with shNS or sh*Klf7* vectors as indicated. Asterisks represent  $p \leq 0.01$  when compared to the indicated control cultures (ANOVA, Scheffè F-test). The lower panel shows the western blot analysis of the KLF7 protein compared to that of  $\beta$ -ACTIN (internal standard).

### 3.3. *Klf7* gene silencing in ES cells.

Using the same experimental paradigm used with PC12 cells, I have generated ES cells stably transfected with shNS or sh*Klf7* vectors. Also in sh*Klf7*-ES stable clones there was a strong decrease of KLF7 protein level (fig. 11a).

Thus to assess whether a KLF7 protein decrease can lead to changes in the ES cells differentiation processes, I have differentiated into neurons shNS-ES and sh*Klf7*-ES stable clones. The major finding was an evident two-days delay in neurites formation in *Klf7*-silenced cells (fig.11c). Moreover, when the *Klf7*-silenced ES cells were induced to differentiate into cardiomyocytes from EBs, there was a dramatic decrease in the beating capacity of cardiomyocytes (fig. 11b).

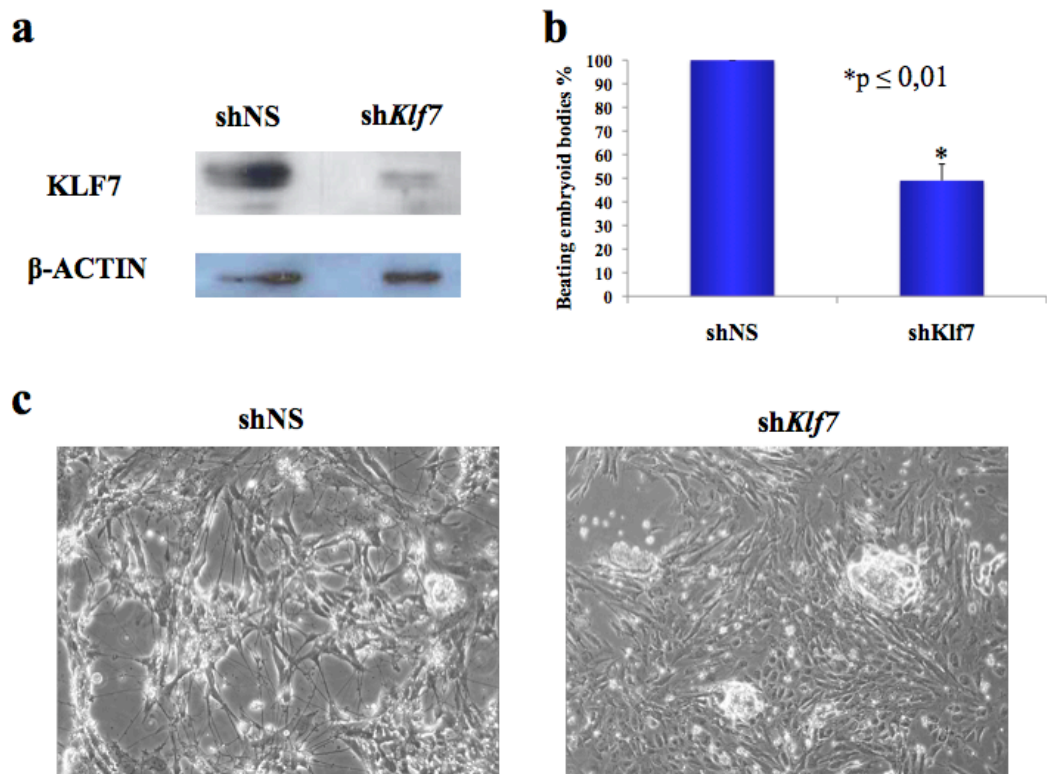


**Figure 11: *Klf7* silencing in ES cells.**

(a) Western blot show KLF7 and ACTIN protein levels in ES cells stably transfected with shNS or sh*Klf7* vectors. (b) Beating ability of cardiomyocytes generated from shNS or sh*Klf7* stably transfected ES cells. Data are expressed as percentage of beating on total EBs. Asterisk represents  $p \leq 0.01$  when compared to control cultures (ANOVA, Scheffè F-test). (c) Neurites outgrowth in shNS or sh*Klf7* stably transfected ES cells following neuronal induction. Images represent cells after 8 days of neuronal induction.

### 3.3.1 KLF7 expression analysis following *Oct4* and *Nanog* gene silencing.

To further analyse KLF7 potential role in ES cells, I have investigated also the possible link between KLF7 and stemness master genes such as *Oct4* and *Nanog*. To this aim I have generated ES stable clones silenced for *Oct4* or *Nanog*, using two shRNA expressing vectors included in the same library of the sh*Klf7* vector. Thus I have induced neuronal differentiation sh*Oct4*-ES or sh*Nanog*-ES stable clones, and analysed the *Klf7* transcriptional changes. The real time RT-PCR analysis showed that in the differentiated cells there was a significant increase of *Klf7* transcripts (fig.12), suggesting that *Oct4* and *Nanog* may have a repression activity on *Klf7* transcription.

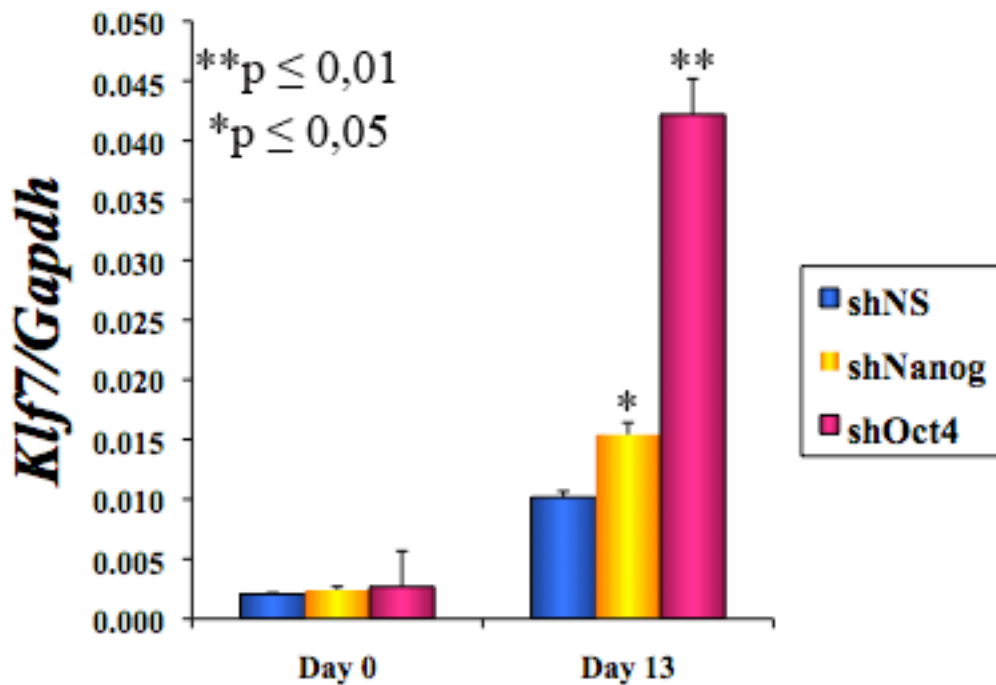


**Figure 12: *Klf7* expression level following *Oct4* or *Nanog* silencing.**

The diagram shows the relative quantization (mean  $\pm$  SE) of the *Klf7* transcript amplified product compared to that of the glyceraldehyde-3-phosphate dehydrogenase (*Gapdh*, internal standard). Data are expressed as ratio *Klf7/Gapdh*. Analyses were performed in ES cells stably transfected with shNS, sh*Nanog* or sh*Oct4* vectors as indicated. Asterisks represent  $p \leq 0.05$  or  $p \leq 0.01$  when compared to the control cultures (ANOVA, Scheffè F-test).

### 3.4 KLF7 role in mesenchymal differentiation.

The results of ES cells based experiments and KLF7 known role in adipogenesis, prompted me to investigate KLF7 possible function in mesenchymal differentiation. It is well known that mesenchymal stem cells (MSC) can differentiate into adipocytes, chondrocytes and osteocytes (Pittenger et al., 1999). In order to analyse mesenchymal pathways following KLF7 deprivation, I have used the *Klf7*-KO mice. Unfortunately it is very problematic to generate MSC from *Klf7*-KO mice bone marrow, since they die perinatally, thus I have used MEF that can be differentiated into adipocytes and osteocytes (Alexander et al., 1998; Garreta et al., 2006).

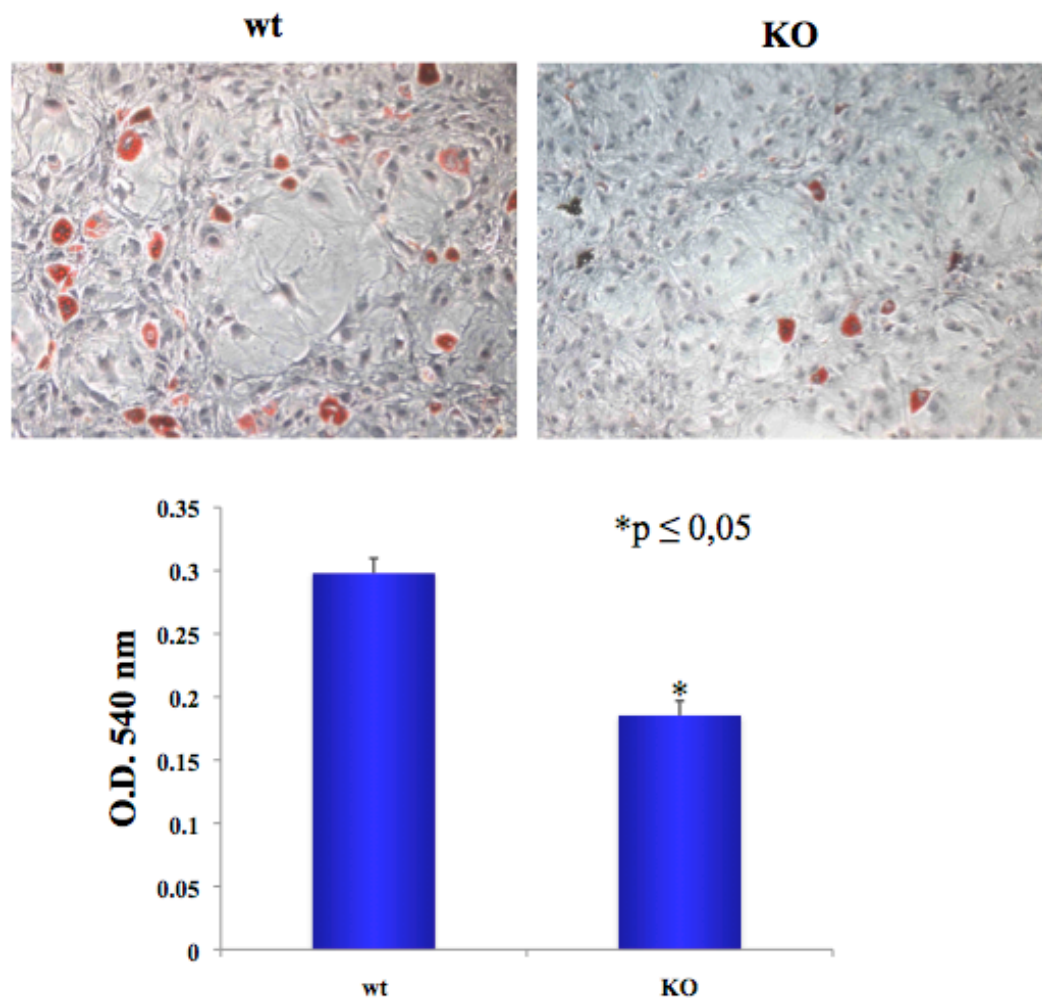


**Figure 13: wt and *Klf7*-KO MEF adipogenic differentiation.**

The upper panels show the Oil Red staining of MEF differentiated into adipocytes. The diagram shows the quantification of the lipids droplets deposits after extraction with isopropyl alcohol. Asterisk represents  $p \leq 0.05$  when compared to wt control cultures (ANOVA, Scheffé F-test).

First I have differentiated MEF derived from wt and *Klf7*-KO mice to adipocytes, and by Oil red staining, I have shown that *Klf7*-KO MEF share a significant decreased adipogenesis (fig. 13).

On the contrary when *Klf7*-KO MEF underwent osteogenic differentiation, have shown a slight increase in the Alizarin red staining, proving increased osteogenesis (fig. 14).

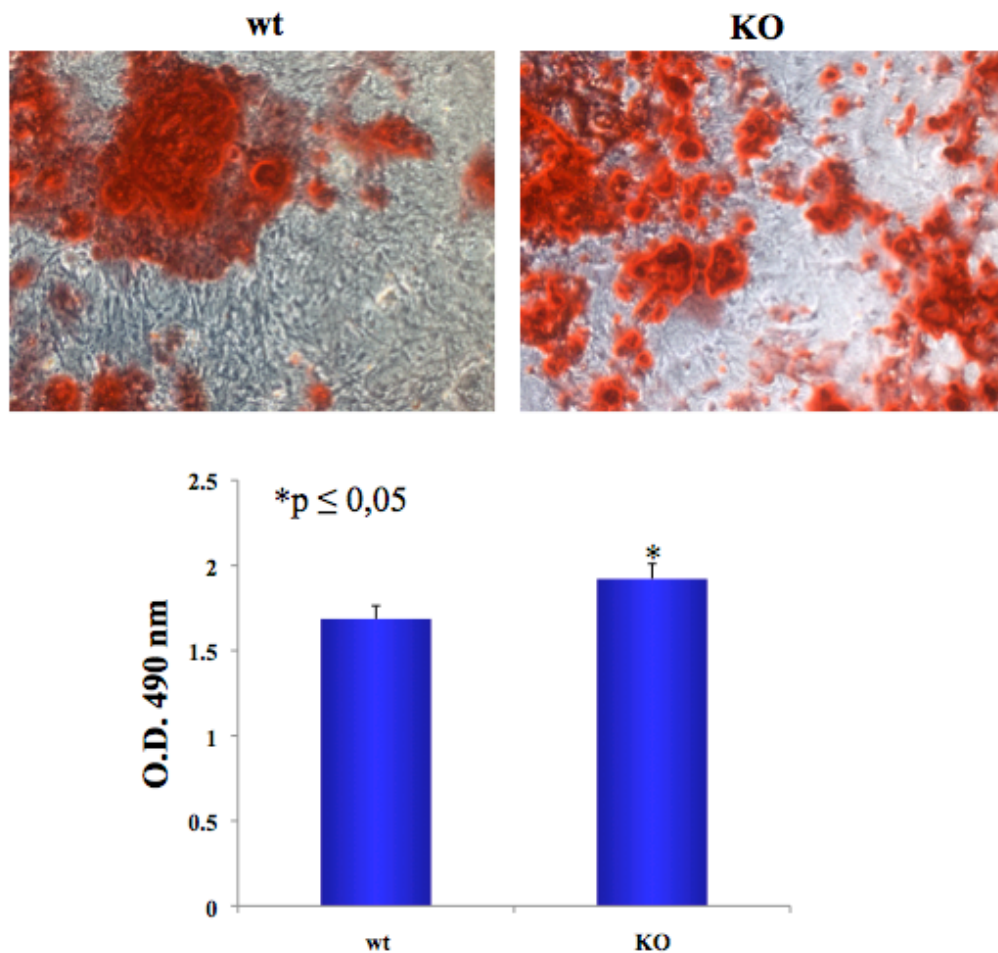


**Figure 14: wt and *Klf7*-KO MEF osteogenic differentiation.**

The upper panels show the Alizarin Red staining of MEF differentiated into osteocytes. The diagram shows the quantification of calcium deposits after extraction with guanidine-HCl. Asterisk represents  $p \leq 0.05$  when compared to wt control cultures (ANOVA, Scheffè F-test).

### 3.5 KLF7 role in NSC.

Previous published works proved with *in vivo* expression data and KO characterization experiments that KLF7 is involved in the nervous system development, but it is not known if it is important for the NSC biology. To this aim I have analysed the self-renewal and differentiation skills of wt and *Klf7*-KO neurospheres, derived from newborn mice.

To investigate KLF7 possible role in NSC self-renewal, I have performed a neurosphere assay on wt and KO cultures. Thus I have cultured a small number of neurospheres in 96 multiwell plates (see material and methods) and counted every week the number of neurospheres generated. After 4 weeks I have not found any significant difference in the rate of neurospheres expansion between wt and KO samples (fig. 15).

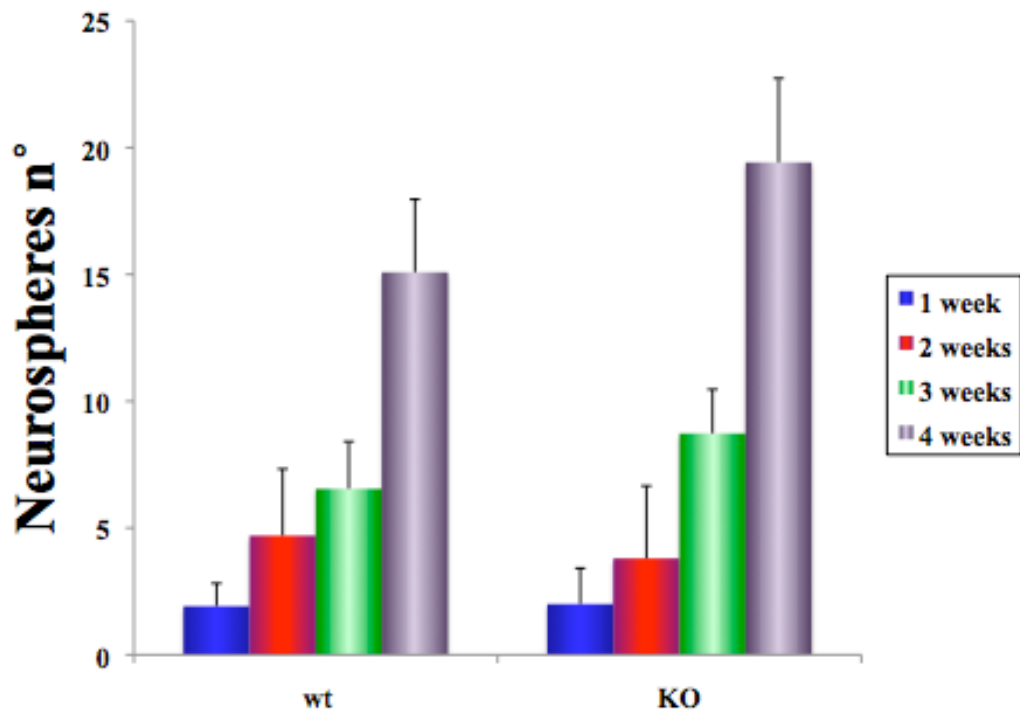


**Figure 15: Self-renewal ability in wt and *Klf7*-KO neurospheres.**

The diagram shows the result of neurospheres assay. Neurospheres have been passed and counted each week.

In parallel I have evaluated the differentiation potential of the wt and *Klf7*-KO dissociated neurospheres into the three neural lineages, namely, neurons, astrocytes and oligodendrocytes. The immunocytochemical analysis have not shown any evident difference in the amount of cells positive for neuronal ( $\beta$ TUBB3), glial (GFAP) or oligodendroglial (NG2) markers after 9 days in culture (fig. 16).

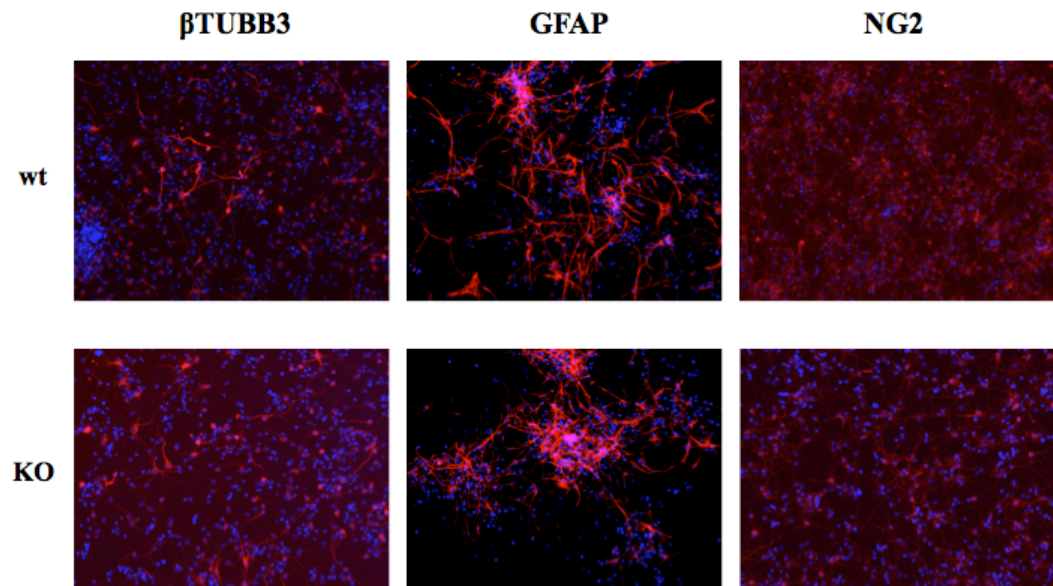


**Figure 16: wt and *Klf7*-KO neurospheres differentiation.**

The panels show immunocytochemical staining on for  $\beta$ TUBB3, GFAP or NG2 on dissociated neurospheres after 9 days of differentiation. The cells nuclei have been stained with DAPI.

Subsequently I have analysed proliferation markers such as Ki67 that marks all mitotically active cells, pospho-HISTONE 3 that highlights only cells in M phase of mitosis, BLBP that is present in all neurogenic regions during brain development and the NSC intermediate filament nestin. Ki67, pospho-HISTONE

3 and nestin immunostaining, did not show differences between wt and *Klf7*-KO samples, whereas I show that *Klf7*-KO cells share a significant decrease in the BLBP positive fraction (fig. 17a,b). Thus I have confirmed by western blot analysis that BLBP protein levels were decreased in the *Klf7*-KO neurospheres derived cells both after 1 day and after 9 days in culture (fig. 17c).

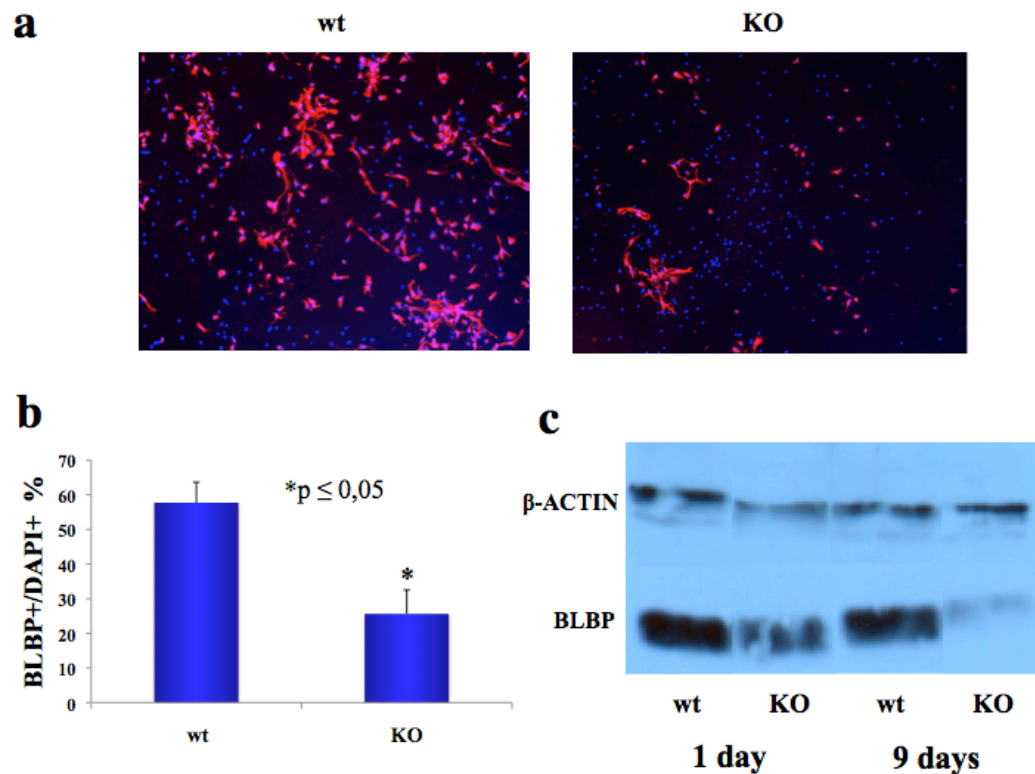


**Figure 17: BLBP protein expression in wt and *Klf7*-KO neurospheres.**

**(a)** BLBP immunohistochemical analysis of dissociated neurospheres after 1 day in culture. The cells nuclei have been stained with DAPI. **(b)** Quantification of BLBP+ cells. Data are expressed as ratio BLBP+/DAPI+ cells. Asterisk represents  $p \leq 0,0505$  when compared to wt control cultures (ANOVA, Scheffè F-test). **(c)** BLBP western blot analysis of dissociated neurospheres after 1 day or 9 days in culture.

In order to understand if the BLBP positive cells overlapped with other NSC markers (nestin, GFAP), I have performed a double staining for BLBP and these

markers, and as it is deductible from the figure 18 both NESTIN and GFAP positive cells were much less than those BLBP positive; moreover in all samples analysed there was not consistent colocalization of BLBP with either NESTIN or GFAP and no evident differences among wt and KO samples. Thus in neurospheres culture BLBP marks a population wider than NSC.

Finally, by real time RT-PCR analysis, I have found that a *Blbp* deficit is present also *in vivo*, at least in *Klf7*-KO OB (fig. 19).

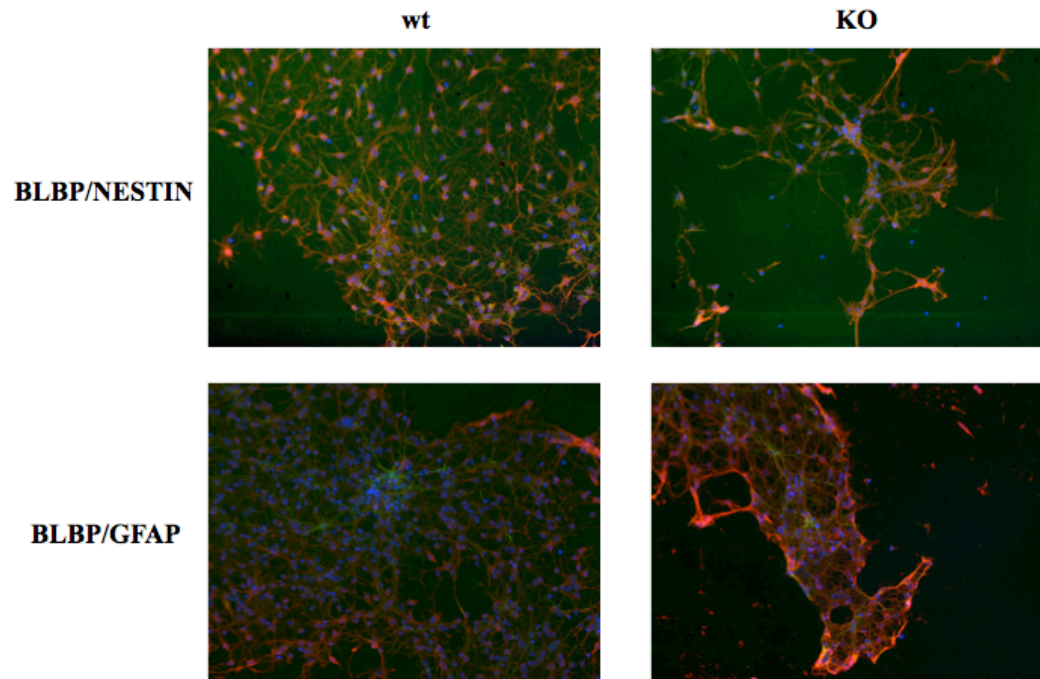


**Figure 18: BLBP+ cells immunocytochemical analysis.**

The panels show the double immunocytochemical staining for BLBP/NESTIN or BLBP/GFAP. BLBP is marked with a rhodaminated secondary antibody, whereas NESTIN and GFAP are marked with a fluorescinated secondary antibody. The cells nuclei have been stained with DAPI.

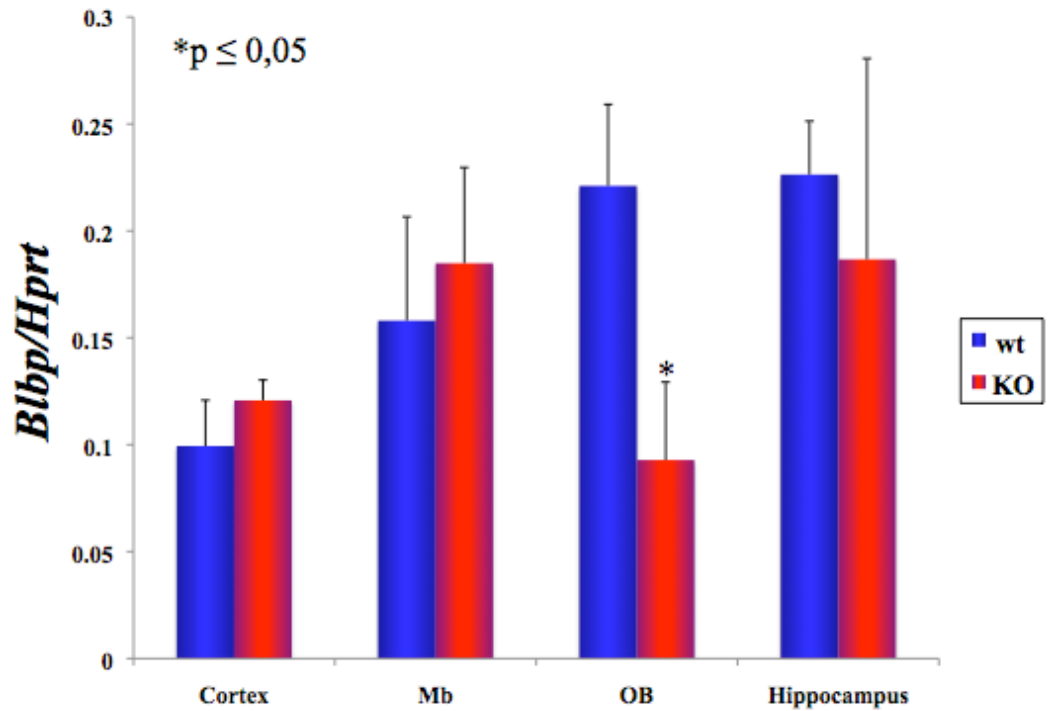


**Figure 19: BLBP transcriptional analysis in newborn brain tissues.**

The diagram shows the relative quantization (mean  $\pm$  SE) of the *Blbp* transcript amplified product compared to that of the *Hypoxanthine phosphoribosyltransferase* (*Hprt*, internal standard). Data are expressed as ratio *Blbp/Hprt*. Asterisk represent  $p \leq 0.05$  when compared to the wt control cultures (ANOVA, Scheffè F-test).

### 3.6 KLF7 role in dopaminergic system development.

Ramirez group has shown by *in situ* experiments, that during CNS development, *Klf7* mRNA is clearly expressed in the ventral Mb between E11,5 and E16,5, that is the same time window in which crucial events for dopaminergic neurons development take place. Thus I have further analysed by real time RT-PCR *Klf7* expression during ventral Mb ontogenesis in wt mouse. This experiment has shown that *Klf7* transcription has a peak between E13,5 and E15,5 that is consistent with a putative role in the development of the Mb dopaminergic system (fig. 20).

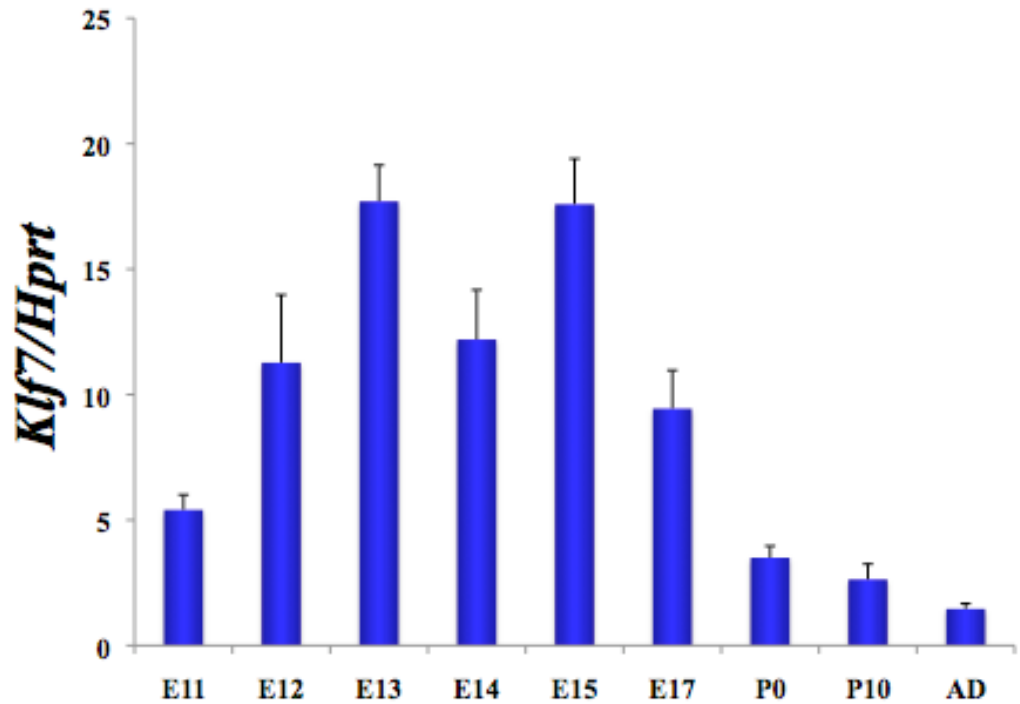


**Figure 20: *Klf7* expression during mouse ventral midbrain ontogeny.**

The diagram shows the relative quantization (mean  $\pm$  SE) of the *Klf7* transcript amplified product compared to that of the *Hypoxanthine phosphoribosyltransferase* (*Hprt*, internal standard). Data are expressed as ratio *Klf7/Hprt*. Additional abbreviations: postnatal day (P), adult stage (AD).

Subsequently to perform a wider characterization of KLF7 role during CNS ontogenesis, I have dissected various brain tissues (cortex, OB, ventral Mb, hippocampus, rombencephalon and spinal cord) from E11,5 to P0 stage derived from wt and *Klf7*-KO mice. These tissues have been analysed by real time RT-PCR with a set of primers for markers of specific neuronal populations and generic markers of development (table 2).

CATEGORY	MARKERS
PRO-NEURAL	<i>Mash1, Ngn1, Ngn1, Neurod</i>
GABAERGIC	<i>Dlx2, Dlx5, Gad1, Gad2, Gat1, Gat2, Gat3, Gat4, Vgat, Gabat.</i>
DOPAMINERGIC	<i>Th, Dat, Nurr1, Pitx3, Vmat2, Lmx1a, Lmx1b, Msx1, Foxa1, Foxa2, En1, En2, Gdnf, Drd1, Drd2, Drd3, Drd4, Drd5.</i>
NORADRENERGIC	<i>Phox2a, Dbh.</i>
SEROTONERGIC	<i>Sert, Tph1, Tph2.</i>
GLUTAMATERGIC	<i>Eaat1.</i>
OTHERS	<i>Map2, Mecp2, Ret, Uncx4.1, Bdnf, TrkA, Otx2, Cacna1a, Cacna1b, Oct4, Nanog.</i>

**Table 2: List of markers analysed in wt and *Klf7*-KO brain tissues.**

Each of the listed markers have been analysed by real time RT-PCR in E11,5; E13,5; E15,5 and P0 wt and *Klf7*-KO brain tissues.

The major findings of the transcriptional analysis have been a significant decrease of *Th* and *Dat* both in the ventral Mb and in the OB of newborn *Klf7*-KO mice. To further analyse if there was a deficit in the differentiation phase of the dopaminergic development, I have also evaluated the expression levels in the ventral Mb of two TFs essential for DA development, *Nurr1* and *Pitx3* and I have not found any significant difference between wt and *Klf7*-KO samples. Also GABAergic (*Gad1*, *Gad2*) and glutamatergic (*Eaat1*) markers, have not shown any transcriptional change in the *Klf7*-KO samples both in the ventral Mb and OB when compared to wt siblings (fig. 21a,b).

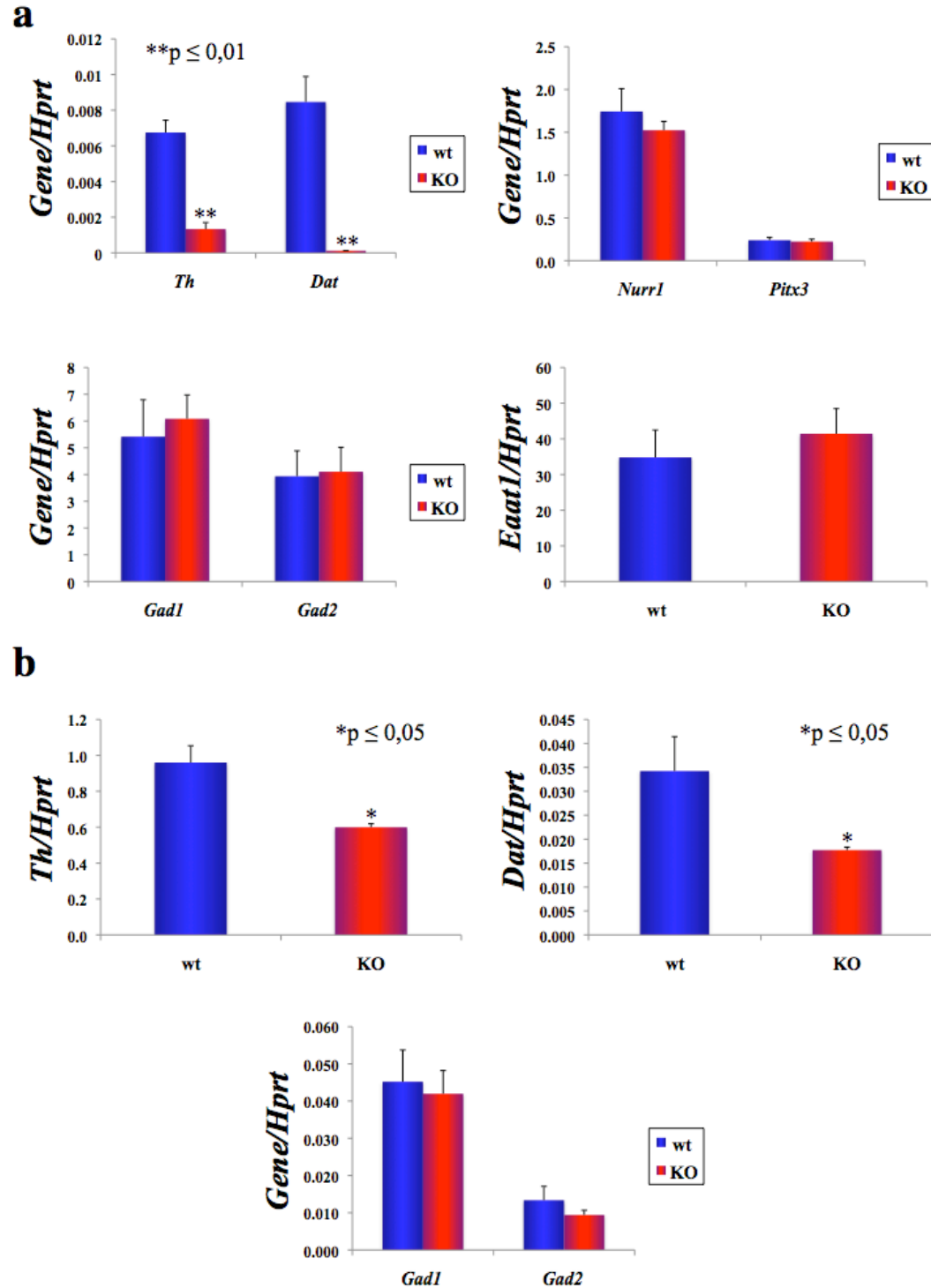


**Figure 21: Transcriptional characterization of wt and *Klf7*-KO ventral Mb and OB.**

The diagrams show the relative quantization (mean  $\pm$  SE) of the *Th*, *Dat*, *Eaat1*, *Gad1* and *Gad2* transcripts amplified product compared to that of the *Hypoxanthine phosphoribosyltransferase* (*Hprt*, internal standard). The analyses were performed on newborn ventral Mb (**a**) or OB (**b**). Data are expressed as ratio *Th/Hprt*, *Dat/Hprt*, *Eaat1/Hprt*, *Gad1/Hprt* or *Gad2/Hprt*. Asterisks represent  $p \leq 0.05$  or  $p \leq 0.01$  when compared to the wt control cultures (ANOVA, Scheffè F-test).

In order to assess the dopaminergic deficit in the *Klf7*-KO brain, I have performed TH immunohistochemical analysis on sagittal brain slices of newborn mice. TH immunostaining highlighted that in the *Klf7*-KO, there is a lighter expression in the ventral Mb, and a drastically impaired signal in the fibers projecting to the *striatum* (fig. 22).

Therefore I have confirmed that KLF7 deprivation during development leads to an impairment of the dopaminergic system, that is particularly evident in the *striatum*.

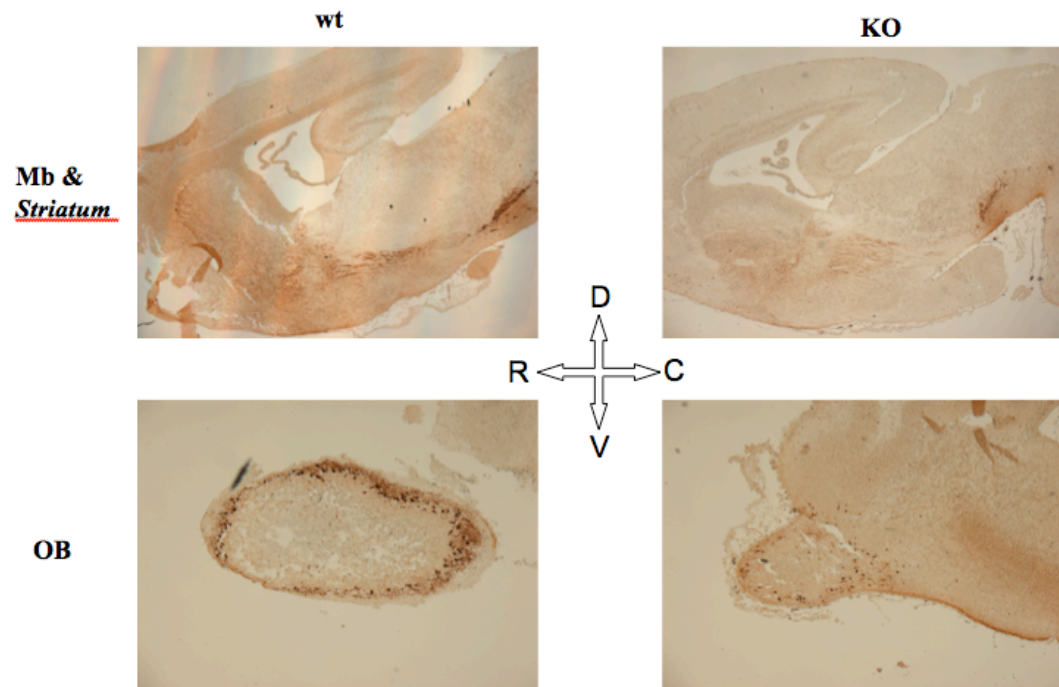


**Figure 22: TH immunohistochemical analysis on wt and *Klf7*-KO brain.**

The panels show TH immunohistochemical staining on sagittal sections. Mb&Striatum and OB images magnification is respectively 2,5x and 5x. The arrows indicate the orientation of the sections: rostral (R), caudal (C), dorsal (D), ventral (V).

**CHAPTER 4**  
**DISCUSSION**

## 4 DISCUSSION

In my PhD project I have studied KLF7 functions both with *in vitro* and *in vivo* approaches.

My *in vitro* experiments have been focused on KLF7 role in cellular differentiation. To this aim I have analysed the possible effects of KLF7 depletion on distinct differentiation processes. Considered that during development *Klf7* is mainly expressed in the nervous system and that it is essential for neuronal development and maintenance in the mouse CNS (Laub et al., 2001, 2005), I have focused my attention predominantly on neuronal differentiation. Thus I have performed *Klf7* RNAi on both the neuronal cell line PC12 and ES cells, and analysed the effects on neuronal markers transcripts or neurite outgrowth.

Downregulation of *Klf7* gene expression in PC12 results in a substantial reduction of *Map2* and *TrkA* transcripts. MAP2 is a well-known hallmark of neuronal differentiation both *in vivo* and *in vitro* (Dehmelt and Halpain, 2004). Thus it is likely that *Klf7* activity may affect *Map2* gene expression by direct or indirect action. Also *TrkA* mRNA strongly decreases following stable silencing of *Klf7* gene expression in PC12 cells. It is well known that PC12 cells differentiate into neurons via stimulation of TRKA, following NGF treatment (Chao and Hempstead, 1995). Moreover this finding is consistent with previously published results showing that KLF7 may activate *TrkA* transcription *in vitro*, and that in *Klf7*-KO mice there is loss of TRKA(+) sensory neurons (Lei et al. 2001, 2005).

*Klf7* silenced ES cells that undergo neuronal induction, share a two days delay in neuronal differentiation, suggesting that KLF7 action is crucial for the right timing of neurites outgrowth. Moreover *Oct4* or *Nanog* silencing by RNAi causes a *Klf7* transcriptional increase in ES cells differentiated into neurons. Thus it is likely that *Klf7* is negatively regulated by *Oct4* and *Nanog*, that is in accordance with published data showing that *Klf7* overexpression in ES cells leads to a differentiated morphology and *Nanog* down-regulation, and that *Klf7* is a potential downstream target of OCT4 and NANOG (Loh et al., 2006, Ivanova et

al. 2006).

The potential KLF7 involvements in ES cells self-renewal mechanisms prompted me to analyse self-renewal and differentiative properties of *Klf7*-KO derived NSC. The neurosphere assay has not shown significant differences between wt and *Klf7*-KO NSC behaviour, but the immunocytochemical and western blot analysis have revealed that the *Klf7*-KO neurospheres share a BLBP protein deficit. It is interesting to note that BLBP is expressed in the neonatal RMS (Hartfuss et al., 2001) as well as *Klf7*, and that in *Klf7*-KO mice there is an evident impairment in the periglomerular layer of the OB, where the neuronal precursors migrating through the RMS differentiate into interneurons (Guillemot and Parras, 2005). Thus it is conceivable that, in *Klf7*-KO mice, BLBP deficit may alter the normal NSC migration along the RMS, during brain development. Further *in vivo* BrdU labeling experiments could clarify this hypothesis.

In order to enrich the functional profile of KLF7 in cellular differentiation, I have also tested its role in other biological processes, such as cardiogenesis, adipogenesis and osteogenesis. Intriguingly I have found that *Klf7* silenced ES cells are strongly impaired to differentiate into cardiomyocytes, whereas in *Klf7*-KO MEF there is an impairment in adipogenic and an increase in the osteogenic differentiation.

Thus *in vitro*, KLF7 seems to have a flexible role in the balance between pluripotency and differentiation induction, depending on the cellular context. A putative example, already mentioned, is that in ES cells OCT4 and NANOG need to repress *Klf7* expression in order to maintain the undifferentiated state.

Another interesting hypothesis about KLF7 role in cellular differentiation is the regulation of mesenchymal pathways. Indeed my experiments show that KLF7 depletion may affect the balance between adipogenesis and osteogenesis in MEF. In contrast with the finding of other groups (Kanazawa et al. 2005, Kawamura et al. 2006) showing that *Klf7* overexpression in preadipocytes inhibits adipogenesis, I find that *Klf7*-KO MEF share impaired adipogenesis. The possible explanation to this apparent contradiction is that during mesenchymal differentiation processes any alteration in the proper KLF7 protein amount can mislead the

differentiative pathways. It is not known if *in vivo* KLF7 is crucial for the regulation of mesenchymal differentiation. Regarding adipogenesis, a partial answer may come from a recently published work that has identified in the *Klf7* promoter a single nucleotide polymorphism that has a protection role against obesity (Zobel et al., 2009).

By *in vivo* analyses, I have focused my attention on the potential KLF7 role in dopaminergic system development. *Klf7* expression in the developing mouse ventral Mb was initially proved by *in situ* experiments (Laub et al., 2001). Thus I have performed a transcriptional characterization of *Klf7* during mouse ventral Mb ontogenesis. The result highlights a peak in *Klf7* transcription between E13,5 and E15,5 suggesting that its expression is needed to fulfil the proper differentiation program of ventral Mb neurons. Moreover the transcriptional analysis of the *Klf7*-KO newborn brain has revealed that dopaminergic markers such as *Th* and *Dat* are impaired both in ventral Mb and OB. The dopaminergic deficit in *Klf7*-KO brain has been further confirmed by immunohistochemical analysis, that also show an impairment of TH protein expression in the nigro-striatal pathway. It is remarkable that I have not found any transcriptional alteration in *Nurr1* and *Pitx3* expression levels, therefore it is likely that KLF7 is not involved in the differentiation phase of dopaminergic neurons, but rather in the maintenance of the dopaminergic phenotype. It is intriguing the hypothesis that in the *Klf7*-KO OB, the dopaminergic and BLBP deficits could be linked. Indeed the OB dopaminergic neurons derive from neuroblasts migrating along the RMS. Considering also the cortex misprojection defects and the *L1cam* deficit in the *Klf7*-KO brain (Laub et al., 2005, Kajimura et al., 2006), it is likely that *in vivo*, *Klf7* role in neuronal morphogenesis is involved in the proper neuronal migration and axonal guidance. The latter are indispensable for the correct neuronal maturation and target recognition, that in turn are crucial for the neurons maintenance and survival. This is well documented for DA neurons (Smidt and Burbach, 2007).

Thus understanding of KLF7 functions may be useful to better comprehend the mechanisms that underlie nervous system developmental processes. Among these,

the maintenance of the dopaminergic phenotype, specially in the nigro-striatal pathway, seems to be affected by KLF7 expression, suggesting a potential involvement in a neurodegenerative disease such as PD.

## **BIBLIOGRAPHY**

**BIBLIOGRAFY**

**Abeliovich A., Hammond R.,** 2007. Midbrain dopamine neuron differentiation: factors and fates. *Dev. Biol.* 304: 447–454.

**Alexander D.L., Ganem L.G., Fernandez-Salguero P., Gonzalez F., Jefcoate C.R.,** 1998. Aryl-hydrocarbon receptor is an inhibitory regulator of lipid synthesis and of commitment to adipogenesis. *J. Cell. Sci.* 111(Pt 22):3311 – 3322.

**Ang S.L.,** 2006. Transcriptional control of midbrain dopaminergic neuron development. *Development* 133: 3499–3506.

**Adams M.D., Celniker S.E., Holt R.A., Evans C.A., Gocayne J.D., Amanatides P.G., Scherer S.E., Li P.W., Hoskins R.A., et al.,** 2000. The genome sequence of *Drosophila melanogaster*. *Science* 287: 2185-95.

**Bayer S.A., Wills K.V., Triarhou L.C., Ghetti B.,** 1995. Time of neuron origin and gradients of neurogenesis in midbrain dopaminergic neurons in the mouse. *Exp. Brain. Res.* 105: 191–199.

**Berg J.M.,** 1988. Proposed structure for the zinc-binding domains from transcription factor IIIA and related proteins. *Proc. Natl. Acad. Sci. U S A.* 85 (1):99-102.

**Berg J.M., Shi Y.,** 1996. The galvanization of biology: a growing appreciation for the roles of zinc. *Science* 271: 1081-1085.

**Bieker J.J.,** 2001. Kruppel-like factors: three fingers in many pies. *J. Biol. Chem.* 276, 34355-34358.

**Björklund A., Dunnett S.B.,** 2007. Dopamine neuron systems in the brain: an update. *Trends Neurosci.* 30: 194–202.

**Boiani M., Scholer H.R.,** 2005. Regulatory networks in embryo-derived pluripotent stem cells. *Nat. Rev. Mol. Cell. Biol.* 6, 872-884.

**Calò L., Spillantini M., Nicoletti F., Allen N.D.,** 2005. Nurr1 co-localizes with EphB1 receptors in the developing ventral midbrain, and its expression is enhanced by the EphB1 ligand, ephrinB2. *J. Neurochem.* 92: 235–245.

**Campos L.S.,** 2004. Neurospheres: Insights Into Neural Stem Cell Biology. *J. Neurosci. Res.* 78(6):761-9.

**Chao M.V., Hempstead B.L.,** 1995. p75 and Trk: a two-receptor system. *Trends Neurosci.* 18, 321-326.

**Chomczynski P., Sacchi N.,** 1987. Single-step method of RNA isolation by acid guanidinium thiocyanate-phenol-chloroform extraction. *Anal. Biochem.* 162(1): 156-9.

**Clarke N.D., Berg J.M.,** 1998. Zinc fingers in *Caenorhabditis elegans*: finding families and probing pathways. *Science* 282: 2018-22.

**De Graeve F., Smaldone S., Laub F., Mlodzik M., Bhat M., Ramirez F.,** 2003. Identification of the *Drosophila* progenitor of mammalian Krüppel-like factors 6 and 7 and a determinant of fly development. *Gene* 314:55-62.

**Dehmelt L., Halpain S.,** 2004. The MAP2/Tau family of microtubule-associated proteins. *Genome Biol.* 6, 204.

**Digirolamo C.M., Stokes D., Colter D., Phinney D.G., Class R, Prockop D.J.,** 1999. Propagation and senescence of human marrow stromal cells in culture: a simple colony-forming assay identifies samples with the greatest potential to propagate and differentiate. *Br. J. Haematol.* 107(2): 275-81.

**di Porzio U., Daguet M.C., Glowinski J., Prochiantz A.,** 1980. Effect of striatal cells on in vitro maturation of mesencephalic dopaminergic neurones grown in serum-free conditions. *Nature* 27; 288(5789):370-3.

**di Porzio U., Zuddas A., Cosenza-Murphy D.B., Barker J.L.,** 1990. Early appearance of tyrosine hydroxylase immunoreactive cells in the mesencephalon of mouse embryos. *Int. J. Dev. Neurosci.* 8: 523–532.

**Doetsch F., Caille I., Lim D. A., Garcia-Verdugo J. M., Alvarez-Buylla A.,** 1999. Subventricular zone astrocytes are neural stem cells in the adult mammalian brain. *Cell* 97, 703–716.

**Fico A., Manganelli G., Simeone M., Guido S., Minchiotti G., Filosa S.,** 2008. High-throughput screening-compatible single-step protocol to differentiate embryonic stem cells in neurons. *Stem Cells Dev.* 17(3):573-84.

**Garreta E., Genové E., Borrós S., Semino C.E.,** 2006. Osteogenic differentiation of mouse embryonic stem cells and mouse embryonic fibroblasts in a three-dimensional self-assembling peptide scaffold. *Tissue Eng.* 12(8):2215-27.

**Goldman, J. E.,** 1995. Lineage, migration, and fate determination of postnatal subventricular zone cells in the mammalian CNS. *J. Neurooncol.* 24, 61–64.

**Götz M.,** 2003. Glial cells generate neurons--master control within CNS regions: developmental perspectives on neural stem cells. *Neuroscientist* 9(5):379-97.

**Götz M., Huttner W.B.,** 2005. The cell biology of neurogenesis. *Nat. Rev. Mol. Cell. Biol.* 6(10): 777-88.

**Guillemot F., Parras C.,** 2005. Adult neurogenesis: a tale of two precursors. *Nat. Neurosci.* 8(7):846-8.

**Hagen G., Muller S, Beato M, Suske G.,** 1992. Cloning by recognition site screening of two novel GT box binding proteins: a family of SP1 related genes. *Nucleic Acids Res.* 20: 5519-5525.

**Hannon R., Evans T, Felsenfeld G, Gould H.,** 1991. Structure and promoter activity of the gene for the erythroid transcription factor GATA-1. *Proc. Natl. Acad. Sci. USA* 88: 3004-3008.

**Hartfuss E., Galli R., Heins N., Götz M.,** 2001. Characterization of CNS precursor subtypes and radial glia. *Dev. Biol.* 229(1):15-30.

**Hoovers J.M., Mannens M, John R, Blik J, van Heyningen V, Porteous DJ, Leschot NJ, Westerveld A, Little PF.et al.,** 1992. High-resolution localization of 69 potential human zinc finger protein genes: a number are clustered. *Genomics* 12 (2):254-63.

**Ivanova N., Dobrin R., Lu R., Kotenko., Levorse., DeCoste C., Shafer X., Lun Y., Lemischka I.R.,** 2006. Dissecting self-renewal in stem cells with RNA interference. *Nature* 442, 533-588.

**Kadonaga J.T., Carner KR, Masiarz FR, Tjian R.,** 1987. Isolation of cDNA encoding transcription factor SP1 and functional analysis of the DNA binding domain. *Cell* 51: 1079-1090.

**Kajimura D., Dragomir C., Ramirez F., Laub F.,** 2006. Identification of genes regulated by transcription factor KLF7 in differentiating olfactory sensory neurons. *Gene* 388(1-2), 34-42.

**Kanazawa A., Kawamura Y., Sekine A., Iida A., Tsunoda T., Kashiwagi A., Tanaka Y., Babazono T., Matsuda M., et al.,** 2005. Single nucleotide polymorphisms in the gene encoding Kruppel-like factor 7 are associated with type 2 diabetes. *Diabetologia* 48, 1315-1322.

**Kawamura Y., Tanaka Y., Kawamori R., Maeda S.,** 2006. Overexpression of Kruppel-like factor 7 regulates adipocytokine gene expressions in human adipocytes and inhibits glucose-induced insulin secretion in pancreatic beta-cell line. *Mol. Endocrinol.* 20, 844-856.

**Kawasaki H., Mizuseki K., Nishikawa S., Kaneko S., Kuwana Y., Nakanishi S., Nishikawa S.I., Sasai Y.,** 2000. Induction of midbrain dopaminergic neurons from ES cells by stromal cell-derived inducing activity. *Neuron* 28, 31-40.

**Keegan L., Gill G., Ptashne M.,** 1986. Separation of DNA binding from the transcription-activating function of a eukaryotic regulatory protein. *Science* 231: 699-704.

**Kim J.G., Hudson L.D.,** 1992. Novel member of the zinc finger superfamily: a C2-HC finger that recognizes a glia-specific gene. *Mol. Cell. Biol.* 12: 5632-5639.

**Kittappa R., Chang W.W., Awatramani R.B., McKay R.D.,** 2007. The foxa2 gene controls the birth and spontaneous degeneration of dopamine neurons in old age. *PLoS Biol.* 5: e325.

**Klug A.,** 1999. Zinc Finger Peptides for the Regulation of Gene Expression. *J. Mol. Biol.*, 293: 215-218.

**Klug A., Schwabe J.W.R.,** 1995. Protein motifs 5. Zinc fingers. *FASEB J.* 9: 597-604.

**Kruger L., Saporta S., Swanson L.W.,** 1995. Photographic atlas of the rat brain: The cell and fiber architecture illustrated in three planes with stereotaxic coordinates. Cambridge University Press.

**Laub F., Aldabe R., Friedrich V. Jr., Ohnishi S., Yoshida T., Ramirez F.,** 2001. Developmental expression of mouse Kruppel-like transcription factor KLF7 suggests a potential role in neurogenesis. *Dev. Biol.* 233, 305-318.

**Laub F., Lei L., Sumiyoshi H., Kajimura D., Dragomir C., Smaldone S., Puche A.C., Petros T.J., Mason C., et al.,** 2005. Transcription factor KLF7 is important for neuronal morphogenesis in selected regions of the nervous system. *Mol. Cell Biol.* 25, 5699-5711.

**Lei L., Ma L., Nef S., Thai T., Parada L.F.,** 2001. mKlf7, a potential transcriptional regulator of TrkA nerve growth factor receptor expression in sensory and sympathetic neurons. *Development* 128, 1147-1158.

**Lei L., Laub F., Lush M., Romero M., Zhou J., Luikart B., Klesse L., Ramirez F., Parada L.F.,** 2005. The zinc finger transcription factor Klf7 is required for TrkA gene expression and development of nociceptive sensory neurons. *Genes Dev.* 19, 1354-1364.

**Loh Y.H., Wu Q., Chew J.L., Vega B., Zhang W., Chen X., Bourque G., George J., Leong B., et al.,** 2006. The Oct4 and Nanog transcription network regulates pluripotency in mouse embryonic stem cells. *Nat. Genet.* 38, 431-440.

**Lois C., Alvarez-Buylla A.,** 1993. Proliferating subventricular zone cells in the adult mammalian forebrain can differentiate into neurons and glia. *Proc. Natl. Acad. Sci. USA* 90, 2074–2077.

**Luskin M.B.,** 1993. Restricted proliferation and migration of postnatally generated neurons derived from the forebrain subventricular zone. *Neuron* 11, 173–189.

**Madden S.L., Rauscher F.J.D.,** 1993. Positive and negative regulation of transcription and cell growth mediated by the EGR family of zinc-finger gene products. *Ann. NY Acad. Sci.* 684: 75-84.

**Maltsev V.A., Rohwedel J., Hescheler J., Wobus A.M.,** 1993. Embryonic stem cells differentiate in vitro into cardiomyocytes representing sinusnodal, atrial and ventricular cell types. *Mech. Dev.* 44, 41-50.

**McKay R.,** 1997. Stem cells in the central nervous system. *Science* 276: 66-71.

**Matsumoto N., Laub F., Aldabe R., Zhang W., Ramirez F., Yoshida T., Terada M.,** 1998. Cloning the cDNA for a new human zinc finger protein defines a group of closely related Kruppel-like transcription factors. *J. Biol. Chem.* 273: 28229-28237.

**Miller I.J., Bieker J.J.,** 1993. A novel, erythroid cell-specific murine transcription factor that binds to the CACCC element and is related to the Krüppel family of nuclear proteins. *Mol. Cell. Biol.* 13:2776-2786.

**Miller J., McLachlan AD, Klug A.,** 1985. Repetitive zinc-binding domains in the protein transcription factor IIIA from *Xenopus* oocytes. *Embo J.* 4: 1609-1614.

**Nuez B., Michalovich D, Bygrave A, Ploemacher R, Grosveld F., 1995.** Defective haematopoiesis in fetal liver resulting from inactivation of the EKLF gene. *Nature* 375:316-318.

**Nusslein-Volhard C., Wieschaus E., 1980.** Mutations affecting segment number and polarity in *Drosophila*. *Nature* 375: 316-318.

**Pelham H.R.B., Brown D.D., 1980.** A specific transcription factor that can bind either the 5S RNA gene or 5S RNA. *Proc. Natl. Acad. Sci. USA* 77:4170-4174.

**Perkins A. C., Sharpe A.H., Orkin SH., 1995.** Lethal  $\beta$ -thalassaemia in mice lacking the erythroid CACCC-transcription factor EKLF. *Nature* 375: 318-322.

**Perrone-Capano C., di Porzio U., 1996.** Epigenetic factors and midbrain dopaminergic neurone development. *Bioessays* 18: 817–824.

**Perrone-Capano C., di Porzio U., 2000.** Genetic and epigenetic control of midbrain dopaminergic neuron development. *Int. J. Dev. Biol.* 44: 679–687.

**Perrone-Capano C., Volpicelli F., di Porzio U., 2008.** The molecular code involved in midbrain dopaminergic neuron development and maintenance. *Rendiconti lincei* 19, 271-290.

**Phinney D.G., Kopen G., Righter W., Webster S., Tremain N., Prockop DJ., 1999.** Donor variation in the growth properties and osteogenic potential of human marrow stromal cells. *J. Cell. Biochem.* 75(3):424-36.

**Pittenger M.F., Mackay A.M., Beck S.C., Jaiswal R.K., Douglas R., Mosca J.D., Moorman M.A., Simonetti D.W., Craig S., Marshak D.R., 1999.** Multilineage potential of adult human mesenchymal stem cells. *Science* 284(5111):143-7.

**Preiss A., Rosenberg U.B., Kienlin A, Seifert E., Jackle H., 1985.** Molecular genetics of Krüppel, a gene required for segmentation of the Drosophila embryo. *Nature* 313: 27-32.

**Prochiantz A., di Porzio U., Kato A., Berger B., Glowinski J., 1979.** In vitro maturation of mesencephalic dopaminergic neurons from mouse embryos is enhanced in presence of their striatal target cells. *Proc. Natl. Acad. Sci. U S A* 76: 5387–5391.

**Rakic P., 2003.** Developmental and evolutionary adaptations of cortical radial glia. *Cereb. Cortex* 13:541–549.

**Reynolds B.A., Tetzlaff W., Weiss S., 1992.** A multipotent EGF-responsive striatal embryonic progenitor cell produces neurons and astrocytes. *J. Neurosci.* 12(11): 4565-74.

**Reynolds, B.A., Weiss, S., 1992.** Generation of neurons and astrocytes from isolated cells of the adult mammalian central nervous system. *Science* 255, 1707–1710.

**Reynolds B.A., Weiss S., 1996.** Clonal and population analyses demonstrate that an EGF-responsive mammalian embryonic CNS precursor is a stem cell. *Dev. Biol.* 175(1):1-13.

**Sherwood N., Timiras S.P.,** 1970. A stereotaxic atlas of the developing rat brain. University of California press.

**Simeone A., Puelles E., Acampora D.,** 2002. The Otx family. *Curr. Opin. Genet. Dev.* 12: 409–415.

**Smaldone S., Laub F., Else C., Dragomir C., Ramirez F.,** 2004. Identification of MoKA, a novel F-box protein that modulates Kruppel-like transcription factor 7 activity. *Mol. Cell. Biol.* 24:1058–1069.

**Smidt M.P., Burbach J.P.,** 2007. How to make a mesodiencephalic dopaminergic neuron. *Nat. Rev. Neurosci.* 8: 21–32.

**Steel M.C., Buckley N.J.,** 1993. Differential regulation of muscarinic receptor mRNA levels in neuroblastoma cells by chronic agonist exposure: a comparative polymerase chain reaction study. *Mol. Pharmacol.* 43:694-701.

**Weiss S., Dunne C., Hewson J., Wohl C., Wheatley M., Peterson A.C., Reynolds B.A.,** 1996. Multipotent CNS stem cells are present in the adult mammalian spinal cord and ventricular neuroaxis. *J Neurosci* 16:7599– 7609.

**Yang V.W.,** 1998. Eukaryotic transcription factors: identification, characterization and functions. *J Nutr.* 128(11): 2045-51.

**Ying Q.L., Stavridis M., Griffiths D., Li M., Smith A.,** 2003. Conversion of embryonic stem cells into neuroectodermal precursors in adherent monoculture. *Nat. Biotechnol.* 21, 183-186.

**Yue Y, Widmer D.A., Halladay A.K., Cerretti D.P., Wagner G.C., Dreyer J.L., Zhou R.,** 1999. Specification of distinct dopaminergic neural pathways: roles of the Eph family receptor EphB1 and ligand ephrin-B2. *J. Neurosci.* 19: 2090–2101.

**Zobel D, Andreasen C, Burgdorf K, Andersson E, Sandbæk A, Lauritzen T, Borch-Johnsen K, Jørgensen T, Maeda S et al.,** 2009. Variation in the gene encoding Kruppel-like factor 7 influences body fat: studies of 14,818 Danes. *Eur J Endocrinol.* 2009 Jan 15 [Epub ahead of print].